Uveitis

25

Xavier Fagan, Weng Onn Chan, Lyndell Lim, and Jagjit S. Gilhotra

Contents

X. Fagan, MBBS, FRANZCO
Northern Eye Consultants, Melbourne, Australia

W.O. Chan, MB, ChB, MPhil • J.S. Gilhotra, MBBS, FRANZCO (✉)
South Australian Institute of Ophthalmology, Royal Adelaide Hospital, Adelaide, Australia
e-mail: jsgilhotra@gmail.com

L. Lim, MBBS, FRANZCO
Centre for Eye Research Australia, Royal Victorian Eye and Ear Hospital and Royal Melbourne Hospital, Melbourne, Australia

25.1 Introduction

Optical coherence tomography (OCT) provides fast, non-contact and reproducible high-resolution imaging of the posterior pole. With improving resolution down to 1 μm and the ability to clearly define anatomical layers, OCT plays an ever-increasing role in the management of uveitis. Diagnostically, the ability to observe alteration in the reflectivity, thickness and retinal architecture is invaluable in understanding the pathophysiology of some uveitic conditions. Whilst there are general agreements on anatomical layer and nomenclature of the inner retinal layers, the same is less so for the outer retinal layers. In 2014, the IN OCT group produced a consensus statement on the four distinct

C.H. Meyer et al. (eds.), *Spectral Domain Optical Coherence Tomography in Macular Diseases*,
DOI 10.1007/978-81-322-3610-8_25

hyper-reflective outer retinal bands (Staurenghi et al. 2014). From the outermost to the innermost are the retinal pigment epithelium (RPE)/Bruch's membrane complex, the interdigitation zone (IZ), the ellipsoid zone (EZ) and the external limiting membrane (ELM) (Staurenghi et al. 2014). The term 'zone' is used when tissues within a region cannot be clearly delineated with current technology. With enhanced depth imaging, choroidal vasculature and thickness can also be both qualitatively and quantitatively measured. This is particularly helpful in uveitic conditions such as Vogt-Koyanagi-Harada (VKH) syndrome, sympathetic ophthalmia (SO), Behcet's disease and choroidal granuloma.

From a management perspective, OCT is useful in documenting longitudinal changes and resolution of complications, e.g. cystoid macular oedema (CMO), subretinal fluid and choroidal neovascular membrane (CNVM). Specific OCT changes associated with uveitic conditions [e.g. hyper-reflectivity of the outer retina seen in acute posterior multifocal placoid pigment epitheliopathy (APMPPE)] often resolve with treatment, making OCT ideal for assessing treatment response. Prognostically, OCT can be used to predict visual outcome. Patients with disruption of EZ and thinning at the fovea are significantly associated with worse visual acuity (Forooghian et al. 2009). It can also be used to detect the presence of vitreomacular traction (VMT), epiretinal membrane (ERM), foveal atrophy and lamellar holes that can adversely affect the visual outcome.

The main limitation of OCT in uveitis is that any hyper-reflective structures will cast shadows and may mask underlying disorder. Additionally, media opacities (e.g. haemorrhage and vitritis) and movement artefacts can significantly degrade image quality. Finally compared to angiography, OCT can be falsely negative in the presence of leakage.

Whilst uveitic condition often presents with nonspecific inflammatory changes (Fig. 25.1), some have distinct manifestations on OCT. The following chapter will aim to highlight some of the prototypical changes associated with uveitic conditions.

25.2 Macular Oedema

Many uveitic conditions may cause vision loss through reactive macular oedema. Three patterns of macular oedema have been described (Markomichelakis et al. 2004):

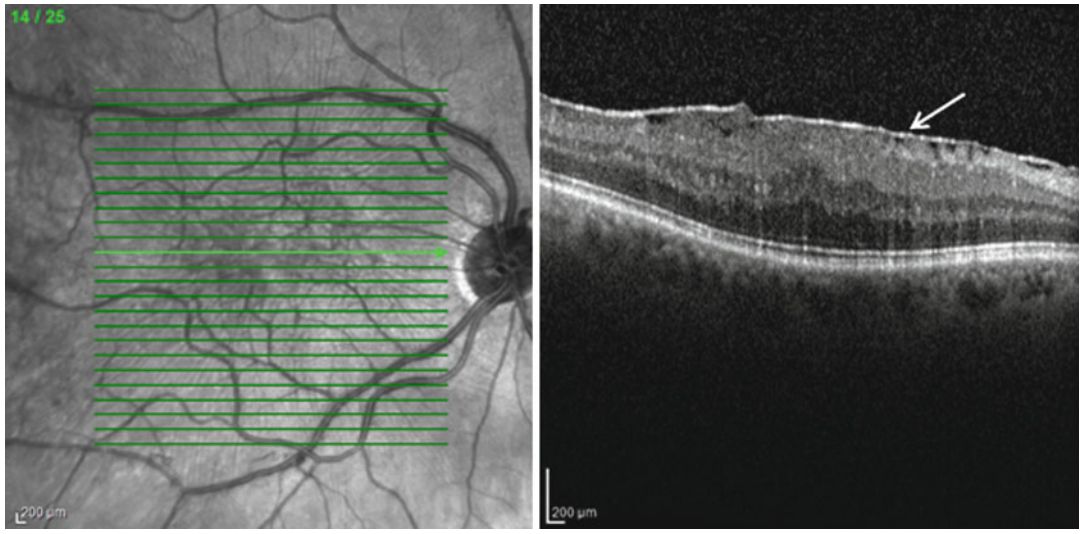

Fig. 25.1 Chronic uveitis. SD-OCT with corresponding red-free showing epiretinal membrane with retinal thickening due to chronic uveitis. The absence of intra-retinal hyporeflective spaces is useful in excluding cystic macular oedema. White arrow pointing to hyper-reflective and thickened epiretinal membrane

1. Diffuse – increased retinal thickness, multiple hyporeflective spaces and separation of retinal lamellae (Fig. 25.2)
2. Cystoid – well-defined intra-retinal cystoid spaces in the retina (Fig. 25.3)
3. Serous detachment – separation of the neurosensory retina from the underlying retinal pigment epithelial-Bruch's membrane complex

Vitreoretinal interface disorders are another potential complications of uveitis and can be seen on OCT as epiretinal membranes, vitreomacular traction or macular hole formation. The ability to detect and measure macular oedema through qualitative and quantitative measures has led to new study designs for the management of uveitic eye disease.

25.3 Idiopathic Inflammatory Chorioretinopathies

25.3.1 Multiple Evanescent White Dot Syndrome (MEWDS)

This transient disorder typically presents in young adults with photopsia and manifests fundoscopically as multiple small, white dots in the

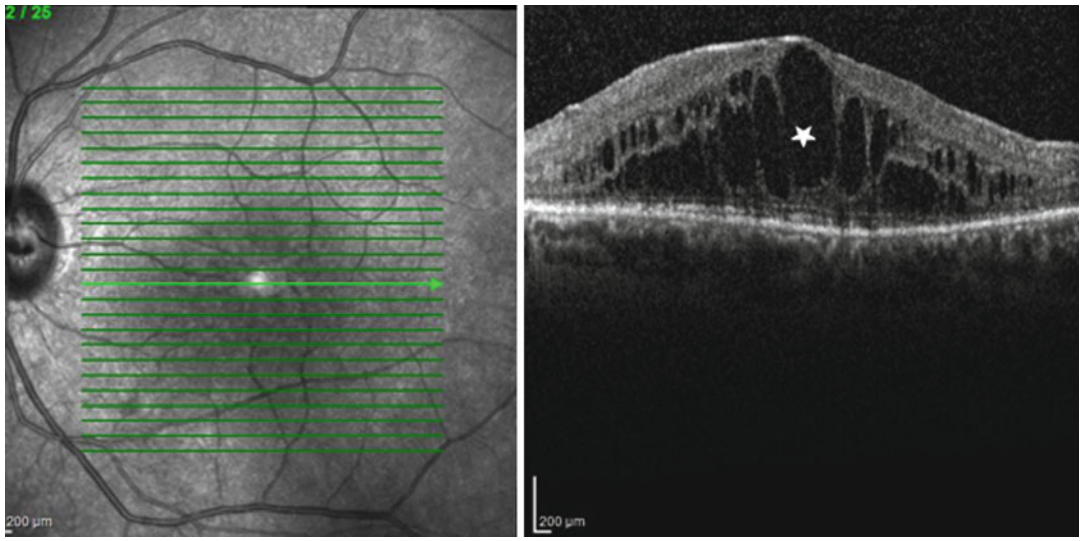

Fig. 25.2 Diffuse cystoid macular oedema (CMO). SD-OCT shows increased retinal thickness with hyporeflective spaces (*white star*) and splitting of the retinal lamellae

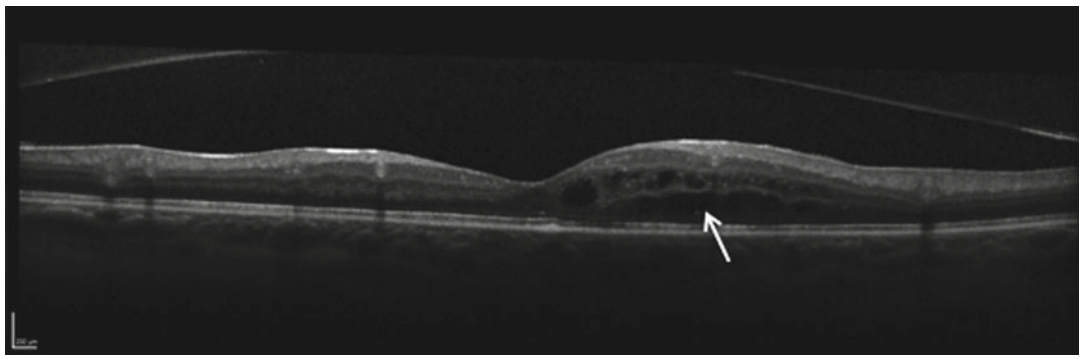

Fig. 25.3 Focal cystoid macular oedema. Focal CMO (*white arrow*) secondary to birdshot choroiditis

posterior pole. Acute presentations demonstrate disruption of the photoreceptor ellipsoid zone (EZ) and interdigitation zone (IZ) (Fig. 25.4a, b) (de Bats et al. 2014; Kanis and van Norren 2006). The disruption may either be diffuse or multifocal. This may be associated with choroidal thickening on enhanced depth imaging OCT (EDI-OCT) and small round hyper-reflective points in other layers such as the ganglion cell layer (de Bats et al. 2014). During follow-up, reconstitution of the EZ occurs gradually over several weeks to months (Li and Kishi 2009) (Fig. 25.5). In some cases, this occurs with an intermediary appearance of small dome-shaped hyper-reflective material that eventually flattens (Amin 2006; Hashimoto and Kishi 2015). En face OCT at the level of the ellipsoid zone may display large patchy areas of hyporeflection corresponding to the diffuse areas of EZ attenuation (de Bats et al. 2014).

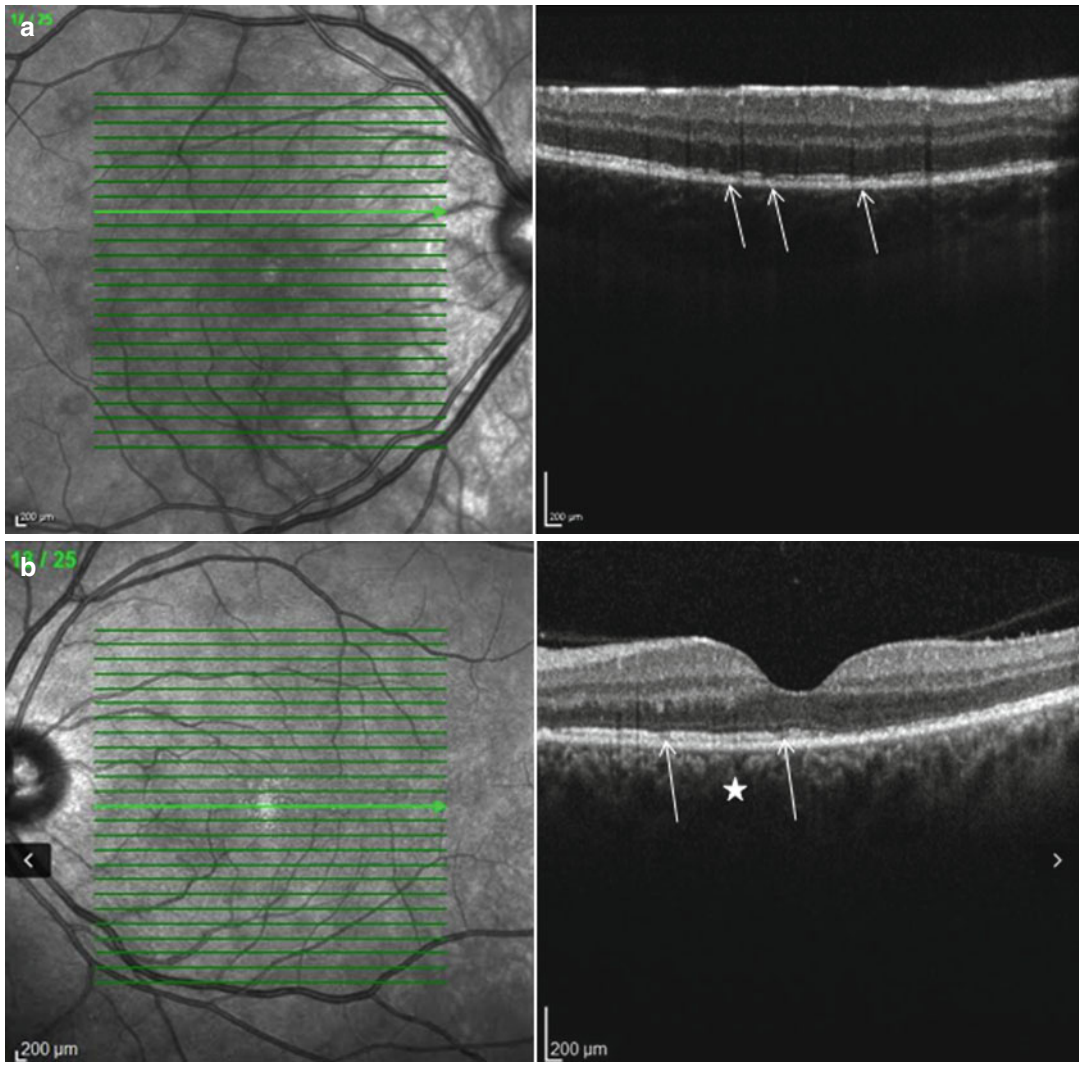

Fig. 25.4 Multiple evanescent white dot syndrome (MEWDS). (**a**) Spectral domain optical coherence tomography (SD-OCT) shows multifocal areas of ellipsoid and interdigitation zone disruption (*white arrows*) corresponding to hyporeflective lesions on the infrared scout map. (**b**) SD-OCT with corresponding red-free showing disruption at the ellipsoid layer (*white arrows*) with associated increased thickness of the choroid (*white star*)

25.3.2 Acute Posterior Multifocal Placoid Pigment Epitheliopathy (APMPPE)

Patients with this acute posterior multifocal placoid pigment epitheliopathy (APMPPE) present with multiple, deep, creamy-white plaques of ½ to 1 disc diameter in size in the posterior pole. Unilateral presentation may also occur. The creamy plaques may be represented on OCT as outer retinal hyper-reflective material with sparing of the middle and inner retina (Scheufele et al. 2005; Souka et al. 2006) (Fig. 25.6). Marked anterior displacement of the neurosensory retina and retinal pigment epithelium (RPE) due to choroidal inflammation may occur (Lim et al. 2006). Areas of turbid subretinal fluid with overlying hyper-reflective material on the RPE (Birnbaum et al. 2010; Lee et al. 2011) and large intra-retinal cysts (Montero et al. 2011) are also described in the acute phase (Fig. 25.7). Serous detachments may be so significant as to mimic Vogt-Koyanagi-Harada disease (Wickremasignhe and Lim 2010). The fluid may become loculated by dividing intra-retinal septa (Lee et al. 2011).

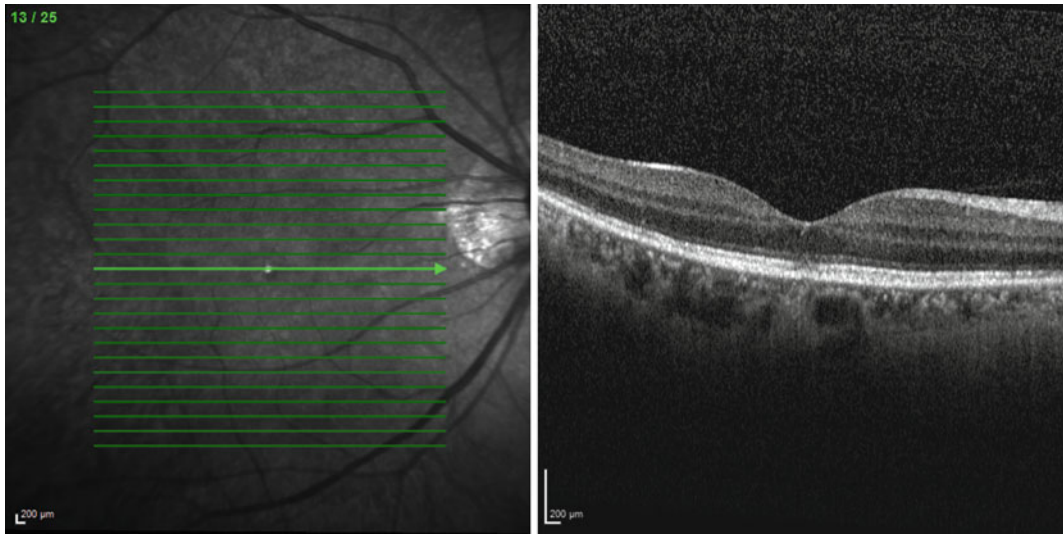

Fig. 25.5 Multiple evanescent white dot syndrome (MEWDS). SD-OCT showing partial reconstitution of the outer retina 2 weeks after onset in a patient with MEWDS

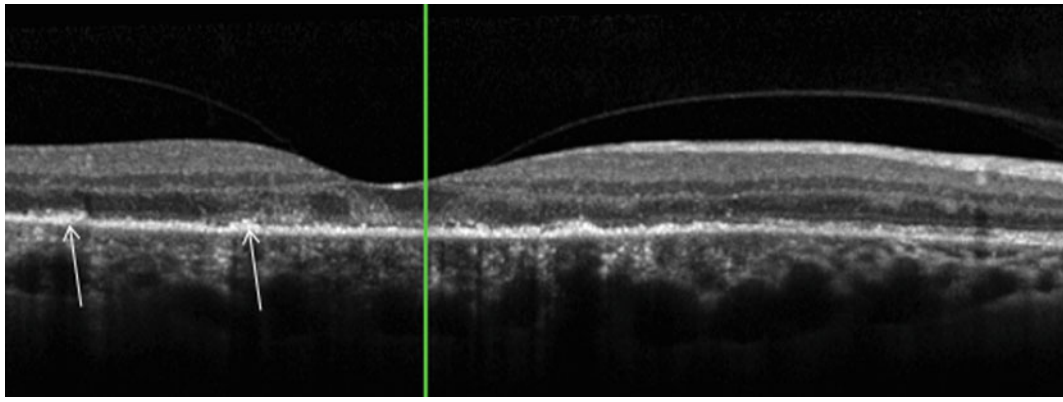

Fig. 25.6 Acute posterior multifocal placoid pigment epitheliopathy (APMPPE). SD-OCT shows outer retinal hyper-reflective material (*white arrows*) and disruption of outer retinal layers. Note sparing of the inner and middle retina

In the convalescent phase, there is rapid resolution of the intra-retinal and subretinal fluid (Birnbaum et al. 2010). This occurs in conjunction with disruption or loss of the IZ, EZ, ELM and outer nuclear layer (ONL). As further repair occurs, there is a variable restoration of outer retinal and RPE elements (Lee et al. 2011) with some cases displaying persistent thinning of the ONL, EZ attenuation and RPE atrophy (Scheufele et al. 2005) (Fig. 25.8).

25.3.3 Relentless Placoid Chorioretinopathy (RPC)

Relentless placoid chorioretinopathy (RPC) also known as ampiginous choroiditis is a related but distinct entity to APMPPE. Whilst initial presentation may be similar, patients with ampiginous choroiditis have prolonged clinical course marred with multiple recurrences. In the acute stages, OCT over the placoid lesions can show pigment epithelial detachment associated with hyperreflectivity of the ganglion cell layer and the inner and the outer nuclear layers (Amer and Florescu 2008) (Fig. 25.9). In the resolution phase, OCT over the placoid scar shows RPE atrophy with associated window defect. However, in contrast to serpiginous chorioretinopathy, retinal and choroidal thickness in RPC is preserved (Dolz-Marco et al. 2014) (Fig. 25.10).

25.3.4 Birdshot Chorioretinopathy

Birdshot chorioretinopathy (BCR) is a typically progressive posterior uveitis characterized by

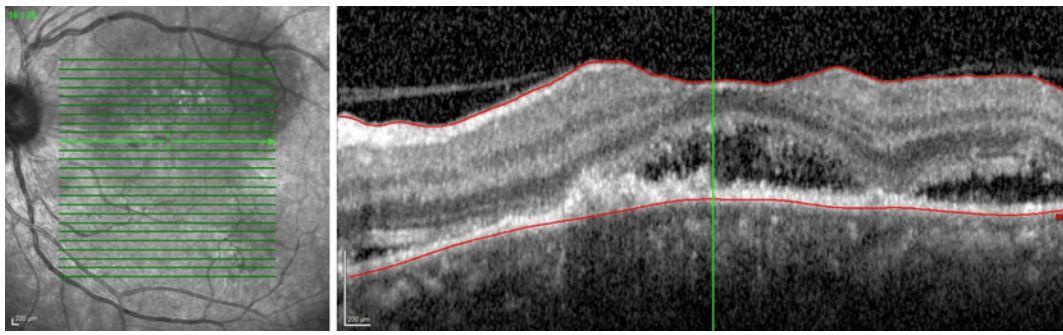

Fig. 25.7 Acute posterior multifocal placoid pigment epitheliopathy. SD-OCT shows subretinal fluid in acute APMPPE

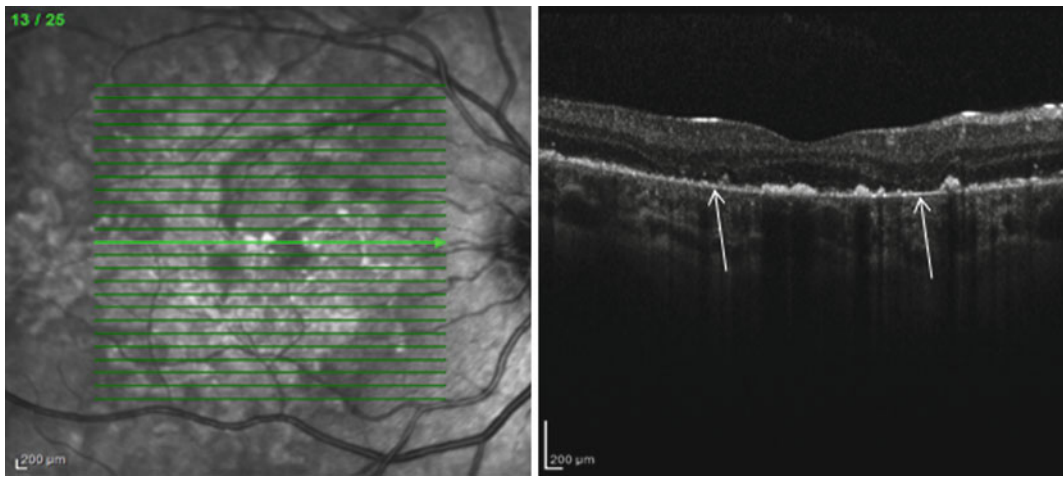

Fig. 25.8 Acute posterior multifocal placoid pigment epitheliopathy. SD-OCT shows loss of outer nuclear layer, interdigitation zone and gross disruption of RPE (*white arrows*) in a patient with previous APMPPE

vitritis, small non-pigmented yellow-white spots predominantly of the nasal fundus and vasculitis and complicated by cystoid macular oedema (CMO). Macular oedema is a common vision-threatening complication of BCR. As described in a previous section, the oedema may be cystoid, diffuse, subretinal fluid or related to epiretinal membrane (Monnet et al. 2007). Classic birdshot lesions can be subtly appreciated as increased transmission of OCT signal to the sclera through the RPE and choroid (Keane et al. 2013) (Fig. 25.11a). Vitritis may be seen as hyper-reflective foci in the lucent background of the vitreous cavity (Fig. 25.11b). Patients with BCR may have suprachoroidal fluid on EDI-OCT (enhanced depth imaging OCT), and there is evidence that the amount of fluid may correlate with photopsias (Birnbaum et al. 2014). Other features include EZ loss, RPE disruption, possible choroidal thinning and outer retinal hyper-reflective

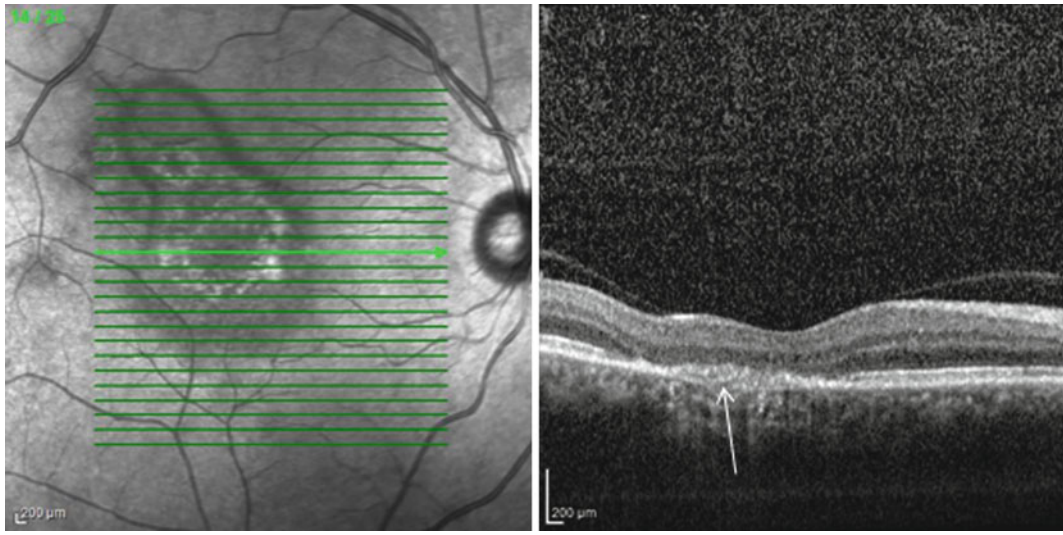

Fig. 25.9 Relentless placoid chorioretinopathy (acute phase). SD-OCT with corresponding red-free showing hyper-reflectivity of the irregular and disrupted outer retinal layers (*white arrow*)

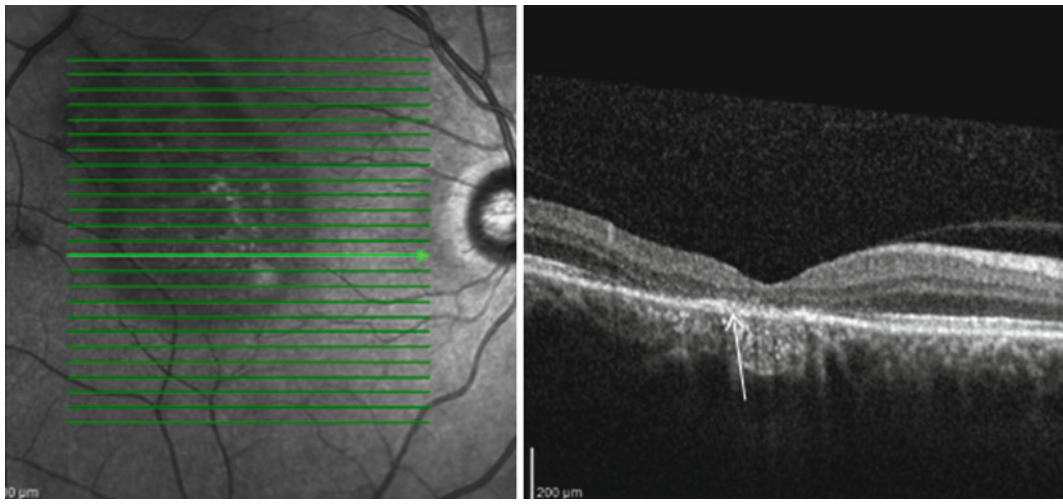

Fig. 25.10 Relentless placoid chorioretinopathy (resolution phase). SD-OCT with corresponding red-free showing disruption at the ellipsoid layer (*white arrow*) in resolution stages of RPC

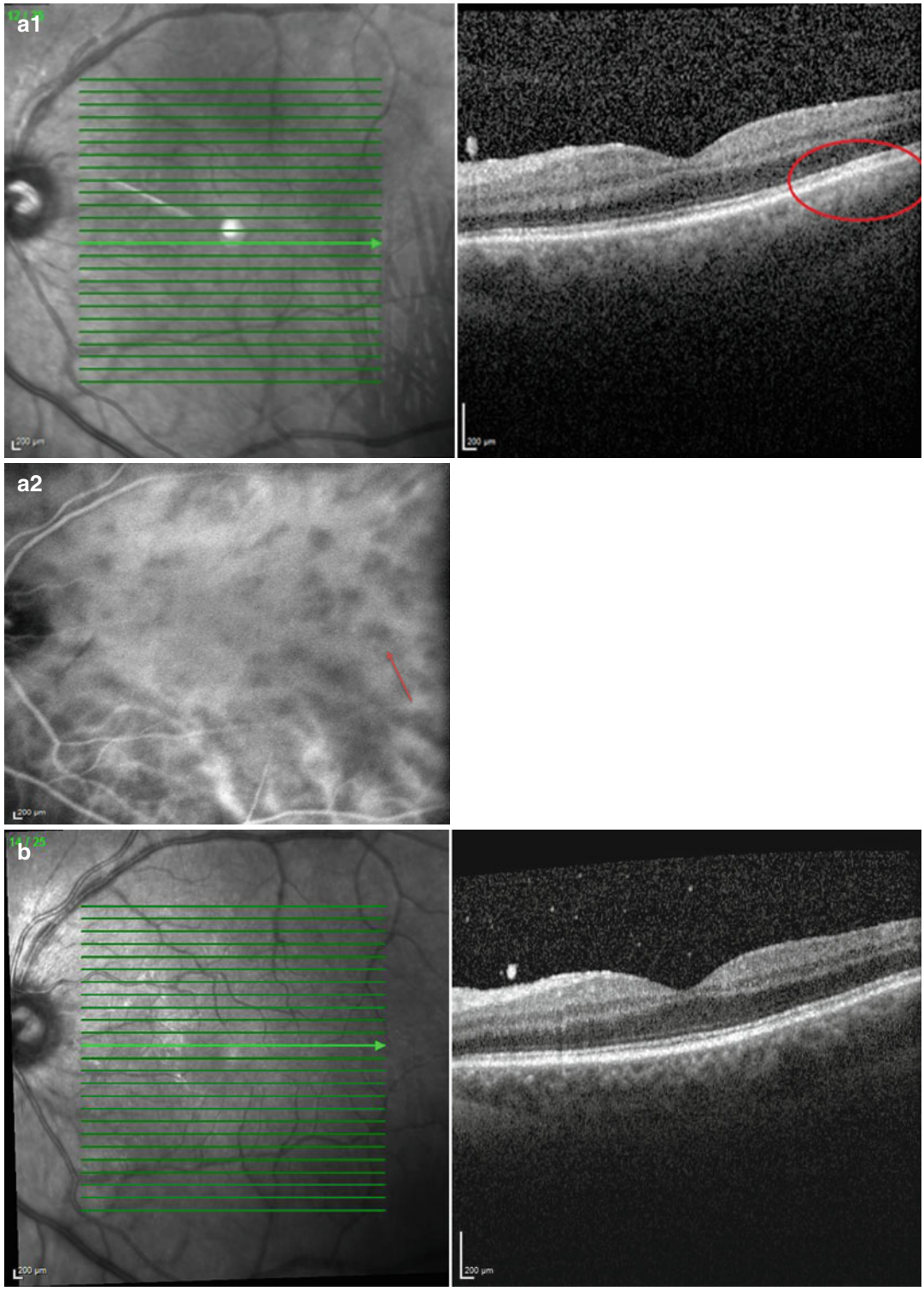

Fig. 25.11 Birdshot chorioretinopathy. (**ai**) SD-OCT with corresponding red-free showing hyper-reflectivity of the outer retinal layers (*red circle*). (**aii**) Indocyanine green angiography (ICG) shows corresponding area as hypofluorescent spot (*red arrow*). (**b**) SD-OCT showing BCR with associated vitritis manifesting as multiple hyper-reflective dots in the vitreous space

lesions or 'clumps' (Keane et al. 2013). Such changes may occur outside the macula and require extra-macular scanning to be detected.

25.3.5 Serpiginous Choroiditis

This disorder is typically characterized by a progressive and recurrent inflammation extending from the optic disc in a centrifugal manner. The active edge of inflammation is a creamy-white colour in the deep layers. The old lesions are seen as atrophic with variable pigment change. It may be complicated by choroidal neovascularization (CNV). Active lesions appear as hyperreflectivities only in the outer retina (van Velthoven et al. 2006), disruption of the EZ and RPE (Arantes et al. 2011) (Fig. 25.12) or cystic macular oedema (Punjabi et al. 2008). En face OCT represents the new inflammation as hyperreflectivity in the outer retina adjacent to the previous inflammation (van Velthoven et al. 2006). Atrophic, chronic lesions are characterized by subsistence of the retina due to loss of outer retinal elements such as the ONL, EZ and RPE (Arantes et al. 2011). Increased transmission through to the choroid is a secondary consequence. Lesions complicated by CNV will display OCT evidence of CNV (Punjabi et al. 2008) depending on the duration of the neovascularization and the involvement of the retina in the primary pathology.

Fundus autofluorescence is a useful adjunctive modality for identifying new lesions as hyperautofluorescent and chronic lesions as hypoautofluorescence or absent autofluorescence (Arantes et al. 2011).

25.3.6 Multifocal Choroiditis with Panuveitis and Punctate Inner Choroidopathy

Previously thought to be separate entities, it has been proffered that punctate inner choroidopathy (PIC) is indistinguishable from multifocal choroiditis (MFC) (Spaide et al. 2013). Both manifest multifocal white-yellow deep infiltrates that may become punched-out scars but had previously been separated by the presence of visible inflammatory cells, lesion size or refractive correction. For the purposes of this section, they will be considered together. Active lesions of MFC may appear as dome-shaped sub-RPE deposits, dehiscence of the RPE, subretinal infiltration and/or loss of the EZ (Channa et al. 2012; Spaide et al. 2013; Vance et al. 2011a). The choroid appears largely uninvolved on multimodal imaging including EDI-OCT (Spaide et al. 2013) but may have increased transmission defects

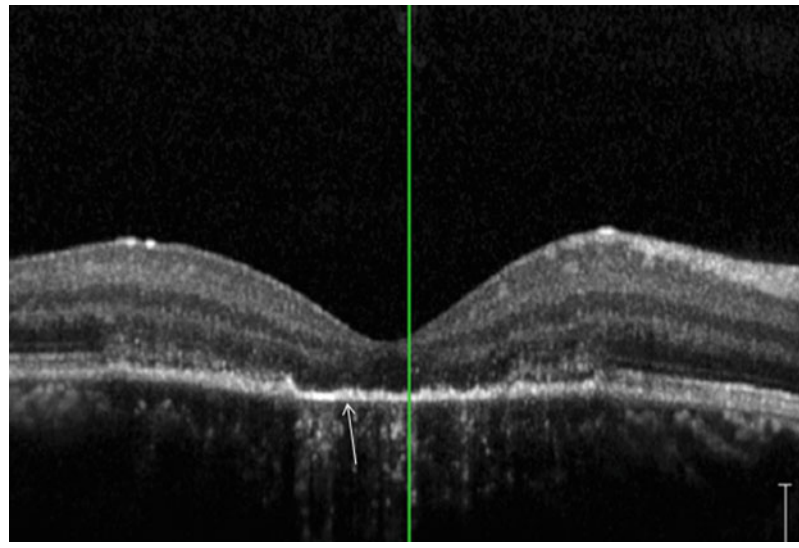

Fig. 25.12 Serpiginous choroiditis. SD-OCT shows active inflammation, seen as hyper-reflective and disturbed outer retinal layers. The more chronic central foveal area has loss of outer retinal layers with increased transmission through to the choroid

from RPE disruption (Vance et al. 2011a, b). Vitreal cells may be visible in the scans. Chronic lesions may show variable presence of the normal outer retinal lamellae or persistent elevation or the absence of the RPE (Channa et al. 2012; Spaide et al. 2013). CNV can complicate MFC and it may be difficult to distinguish it from a new acute MFC lesion. CNV may be associated with subretinal heterogeneous material and round hyporeflective structures suggestive of a vascular lumen (Spaide et al. 2013) (Fig. 25.13).

25.3.7 Acute Macular Neuroretinopathy (AMN)

Prior to OCT and infrared imaging, this condition was clinically detected as subtle, lobular macular red-brown retinal lesions in patients presenting with paracentral scotomas.

There are two subtypes of OCT appearance of acute macular neuroretinopathy (AMN):

A. Outer retinal AMN (Fig. 25.14)
B. Middle maculopathy (Fig. 25.15)

A. Outer retinal AMN was the first to be demonstrated with OCT. Time-domain OCT in the acute presentation showed hyper-reflectivity of the outer retina (Feigl and Haas 2000). On spectral domain OCT (SD-OCT) in the very early presentation, there may be outer retinal hyper-reflectivity followed by focal EZ, IZ and RPE disruption and ONL thinning on spectral domain machines (Monson et al. 2007; Fawzi et al. 2012; Hughes et al. 2009). The EZ re-establishes over time as the condition improves, but ONL thinning and IZ hyporeflectivity thinning may persist (Fawzi et al. 2012; Vance et al. 2011b).

B. Middle maculopathy was identified later in patients with the same demographics, clinical symptoms, fundoscopic findings and infrared reflectance patterns. OCT shows hyper-reflectivity of the INL with shadowing of

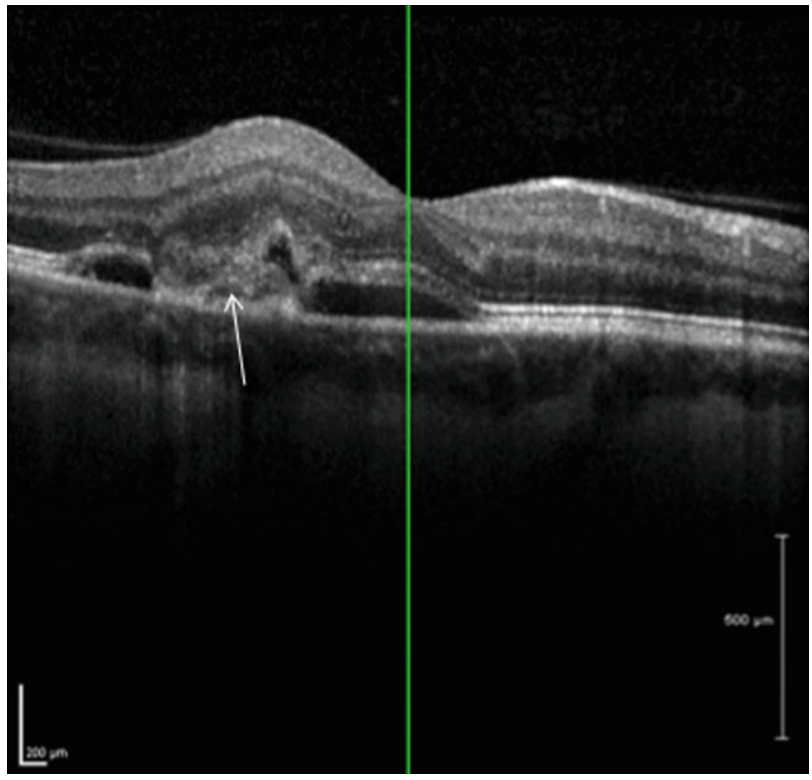

Fig. 25.13 Multifocal choroiditis. Choroidal neovascularization (CNV) (*white arrow*) complicating an old multifocal choroiditis (MFC) lesion. Note the subretinal fluid and heterogeneous material

deeper structures but no focal attenuation (Sarraf et al. 2013). Convalescent images displayed subsequent atrophy of the INL (Sarraf et al. 2013). Whilst it was originally thought that this middle maculopathy might be pathognomonic, it has since been demonstrated in retinal artery occlusion, central retinal vein occlusion, prolonged globe compression and haemoglobinopathies such as sickle cell disease, retinal vasculitis and Purtscher-like retinopathy (Chen et al. 2015; Rahimy et al. 2014; Yu et al. 2015).

It has been postulated that these two patterns represent capillary ischaemia from interruption of the superficial (inner) retinal capillary plexus or deep (outer) retinal capillary plexus (Yu et al. 2014).

25.3.8 Acute Zonal Occult Outer Retinopathy (AZOOR)

The definition of AZOOR is variable. This section refers to otherwise well patients with an initial presentation of photopsia or diminished night

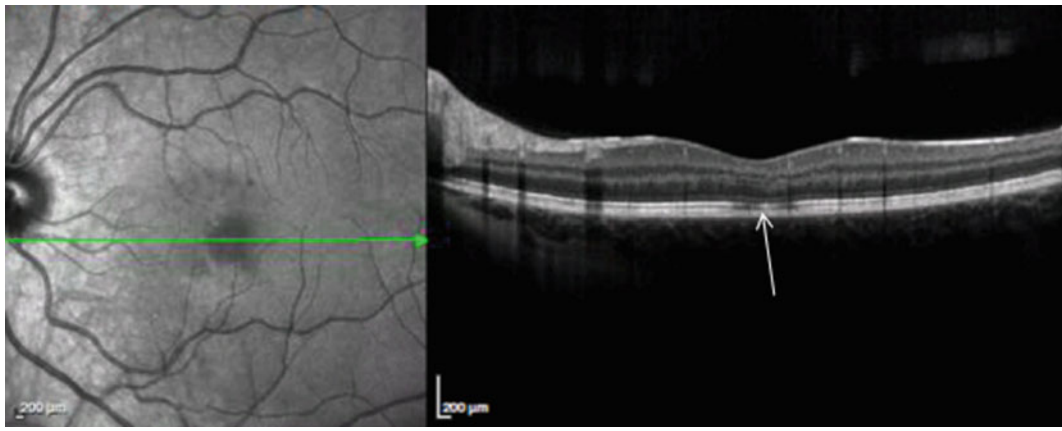

Fig. 25.14 Outer retinal acute macular neuroretinopathy. SD-OCT shows discontinuity of the EZ (*white arrow*) in the central macular area which corresponds to an area of decreased reflectivity on the infrared scout map

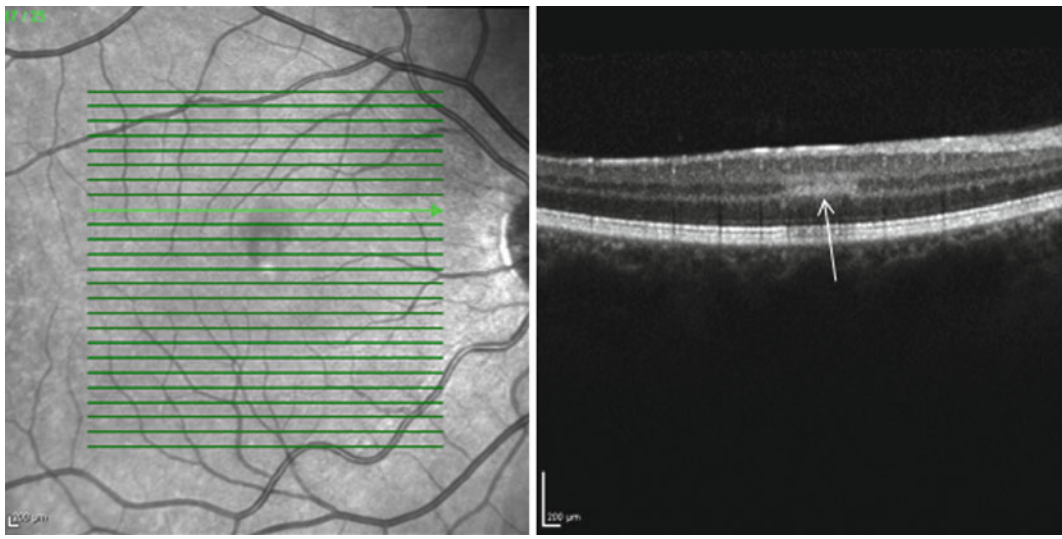

Fig. 25.15 Middle retina acute macular neuroretinopathy. SD-OCT shows hyper-reflectivity in the inner nuclear layer (*white arrow*) and corresponding to an area of decreased infrared reflectance on the scout map

vision, well-defined scotoma or enlarged blind spot without any visible fundus abnormality or features consistent with alternative diagnoses.

OCT in the acute phase shows diffuse loss of ellipsoid zone and interdigitation zone in the involved area as determined by ERG, visual field or autofluorescence (Li and Kishi 2007; Mrejen et al. 2014). Treatment with local or systemic immune suppression has been shown to promote at least partial reconstitution of these lamellae in areas with intact outer nuclear layers (Spaide et al. 2008).

In the chronic phase, patients develop a trizonal appearance with normal OCT outside the area of AZOOR, subretinal material in active areas and atrophy of photoreceptors, RPE and choroid in the chronic areas (Mrejen et al. 2014). Other studies with EDI-OCT report that choroidal thickness is unaffected but confirm the attenuation of the ellipsoid zone and reduced or absent outer nuclear layer (Fujiwara et al. 2010). Epiretinal membrane is common (Fujiwara et al. 2010).

25.3.9 Sarcoidosis

Sarcoidosis is a multisystem, idiopathic, non-caseating granulomatous disease. It may affect the anterior segment, retina, optic nerve or choroid. On OCT imaging, retinal and optic nerve head granulomas appear as inner retinal, hyperreflective nodules protruding into the vitreous (Goldberg et al. 2015). The surrounding tissue is disturbed; there is reduced signal transmission to outer retinal structures, and there may be subretinal fluid (Goldberg et al. 2015). Lesions regress but may not ever completely dissolve (Goldberg et al. 2015). Choroidal granulomas may be identified on EDI-OCT as homogenous lesions that may be isoreflective or hyporeflective relative to the surrounding choroid (Invernizzi et al. 2015; Rostaqui et al. 2014). The overlying choriocapillaris is compressed (Modi et al. 2013). The lesions may be round or lobulated and only half will have well-defined margins (Invernizzi et al. 2015).

25.3.10 Vogt-Koyanagi-Harada (VKH) Syndrome and Sympathetic Ophthalmia

Given their clinical, ophthalmological, histopathological and imaging similarities, these two conditions shall be discussed together in the context of OCT appearance. Choroidal thickening, an undulating RPE and serous retinal detachments characterize the acute phase (Figs. 25.16

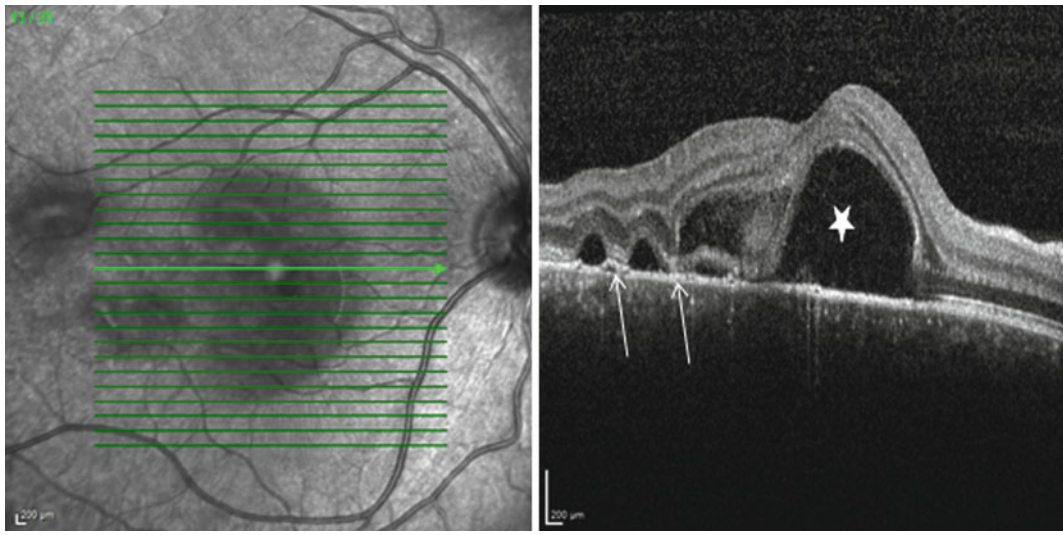

Fig. 25.16 Acute Vogt-Koyanagi-Harada (VKH) syndrome. SD-OCT shows serous detachment of the retina (*white star*) and loculated intra-retinal fluid divided by subretinal strands (*white arrows*)

and 25.17) (Fong et al. 2011; Ishihara et al. 2009). Wavy, hyper-reflective lines traversing and bridging the entirety of the subretinal fluid pockets can be seen (Tsjuikawa et al. 2005). These may represent fibrinous septa (de Smet and Rao 2005) and are responsible for the loculation of fluid compartments seen on fluorescein fundus angiography (FFA) (Yamaguchi et al. 2007). The EZ may be thickened and irregular (Gupta et al. 2009). Hyper-reflective dots, potentially representing small vessels of the choriocapillaris that are present in normal EDI-OCT, have been shown to be less numerous in the acute stage of disease (Fong et al. 2011). Single-layer RPE analysis demonstrates small elevations that correspond to areas of punctate hyperfluorescence on FFA, and troughs in the RPE correspond to hypofluorescent lines on FFA (Gupta et al. 2009). Within a week of steroid therapy, serous retinal detachment starts to resolve (Fig. 25.18), and by 1 month, 75 % of detachments are completely resolved (Ishihara et al. 2009). EZ integrity is reconstituted more gradually and may take 3 months (Ishihara et al. 2009). In the convalescent phase, there is marked, rapid reduction in the choroidal thickness to normal levels after initiation of steroid therapy within 3–14 days (Maruko et al. 2011). In chronic cases of VKH, the choroid is likely to be thinner than control eyes (da Silva et al. 2013). It may be possible to use EDI-OCT measurements of choroidal thickness to gauge treatment response or disease recurrence. Dalen-Fuchs nodules that are seen with both conditions have previously been characterized histologically into three types (Reynard et al. 1985). Type 1 consists of focal hyperplasia and aggregation of RPE cells. Type 2 consists of epithelioid cells and lymphocytes covered by intact dome of RPE. Type 3 consists of degeneration of RPE and release of disorganized Dalen-Fuchs nodule into the subretinal space. With SD-OCT, it is possible to distinguish between the types; however the clinical significance of the different types remains unclear (Figs. 25.19 and 25.20).

25.4 Infectious Posterior Uveitis

25.4.1 Bacterial Posterior Uveitis

25.4.1.1 Acute Syphilitic Posterior Placoid Chorioretinitis

In the acute phase of a macular placoid syphilitic lesion, the OCT demonstrates disruption or loss of the EZ and ELM (Brito et al. 2011) (Fig. 25.21). There may also be subretinal fluid (Joseph et al. 2007; Pichi et al. 2014). The choroid can appear infiltrated with hyper-reflective dots and reduction in the number and size of visible vascular structures (Brito et al. 2011; Pichi et al. 2014).

As the condition is treated, prominent nodular elevations of the RPE are seen (Pichi et al. 2014). After treatment is completed, the subretinal fluid resolves, and the normal foveal lamination is restored (Brito et al. 2011; Joseph et al. 2007; Pichi et al. 2014) (Fig. 25.22). The choroidal infiltration also resolves (Pichi et al. 2014). Rare

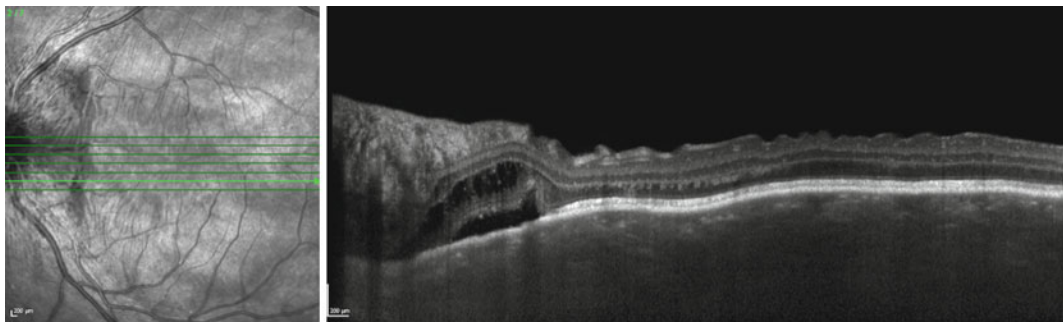

Fig. 25.17 Acute Vogt-Koyanagi-Harada syndrome. EDI-OCT shows a grossly thickened choroid in a patient with acute VKH

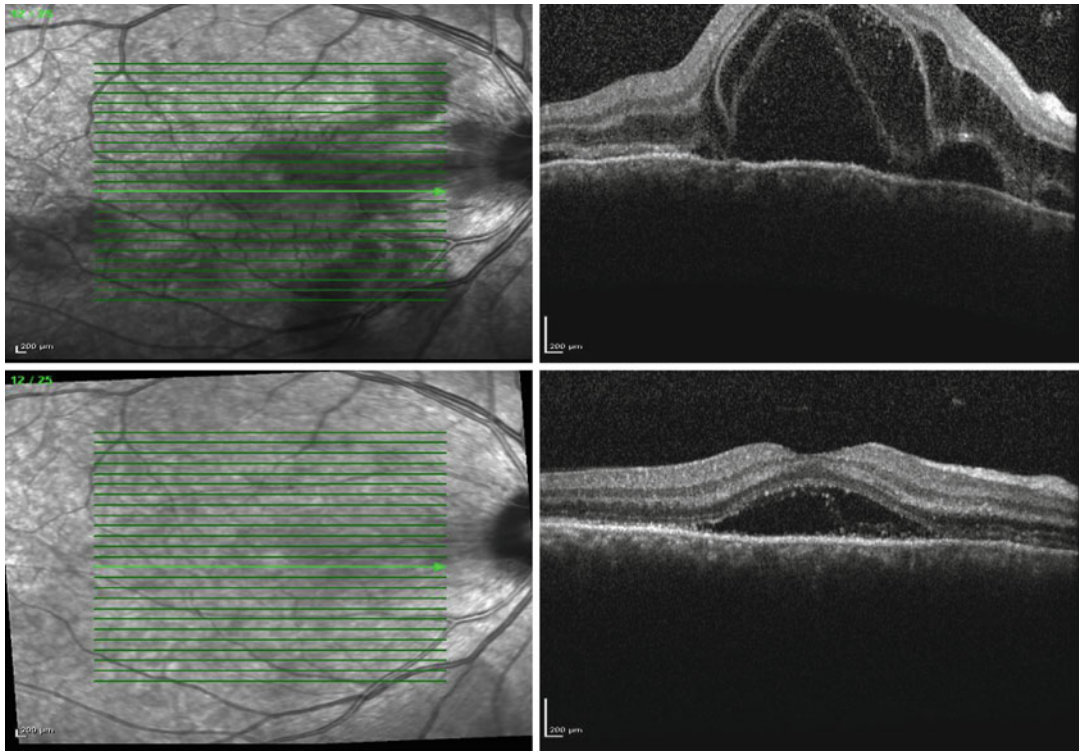

Fig. 25.18 Acute Vogt-Koyanagi-Harada (VKH) syndrome. Acute VKH at presentation and after 3 days of intravenous methylprednisolone. A dramatic reduction in the intra-retinal fluid and retinal thickening is seen

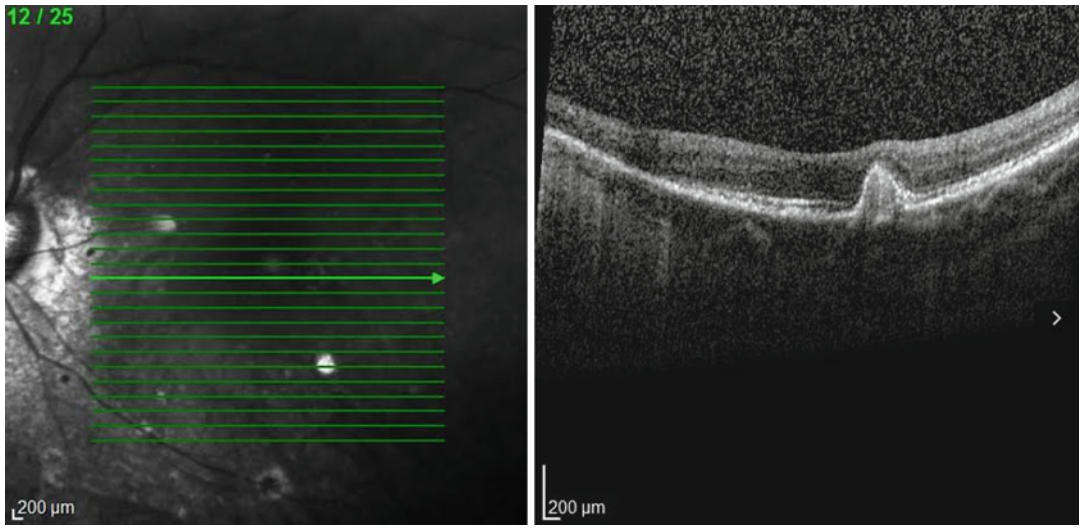

Fig. 25.19 Vogt-Koyanagi-Harada (VKH) syndrome. SD-OCT with corresponding red-free showing type 2 Dalen-Fuchs nodules. Here the dome-shaped elevation has displaced but not disrupted the overlying RPE

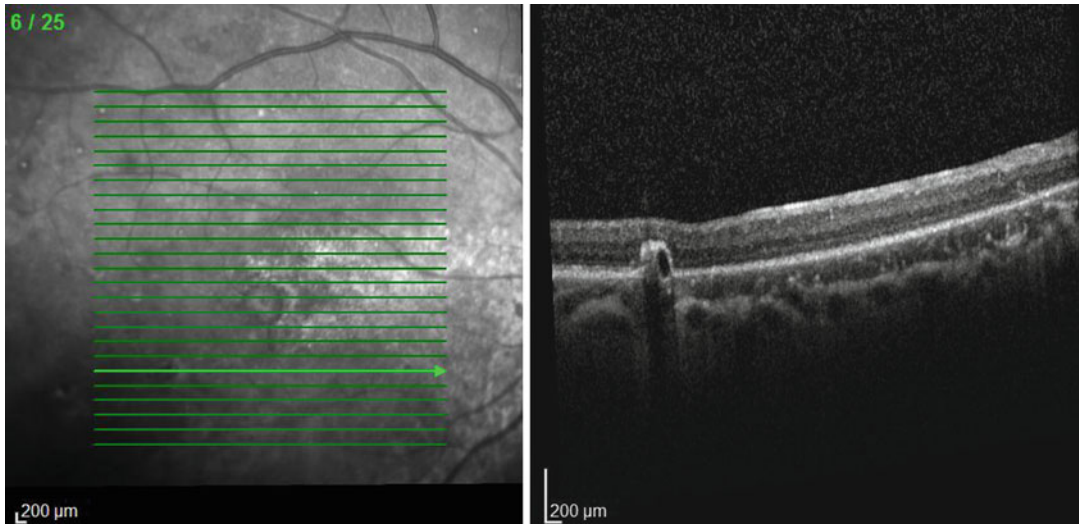

Fig. 25.20 Vogt-Koyanagi-Harada (VKH) syndrome. SD-OCT with corresponding red-free of the right eye showing type 3 Dalen-Fuchs nodule, a dome-shaped elevation that is associated with disruption of overlying retinal pigment epithelial layer

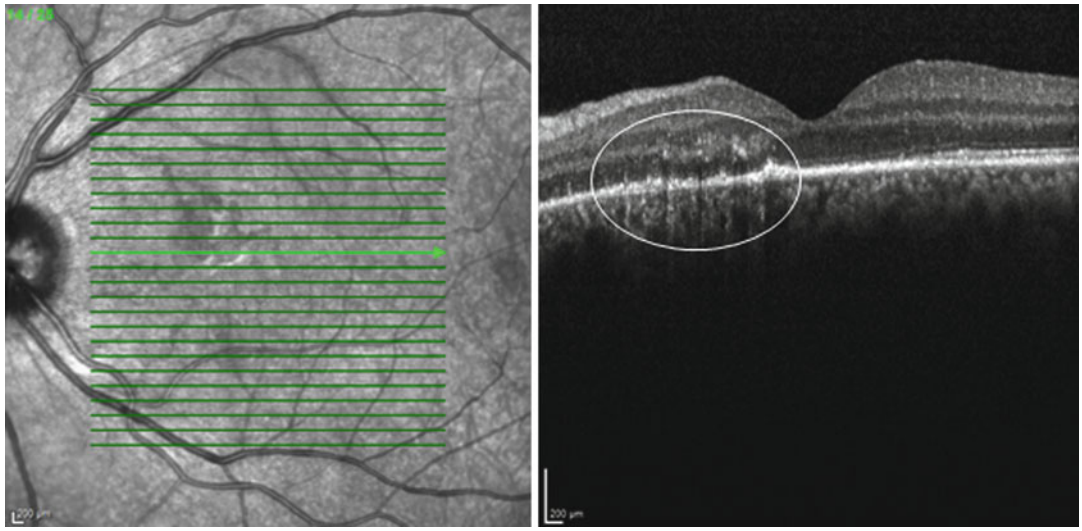

Fig. 25.21 Acute syphilitic posterior placoid chorioretinitis. SD-OCT shows loss of the outer retinal elements and an infiltrated appearance to the choroid (*white circle*)

cases may fail to recover normal foveal anatomy and are associated with a worse final acuity (Pichi et al. 2014).

25.4.1.2 Tuberculous Chorioretinitis

The principal difficulty with tuberculous (TB) uveitis is the confirmation of a case. As such, the literature contains many potential or probable cases rather than definite cases. The OCT imaging itself is therefore coupled with this diagnostic uncertainty, and there are no proven pathognomonic imaging features. The following paragraphs describe the various clinical appearances ascribed to TB uveitis and the corresponding imaging.

A. Focal TB chorioretinitis
   A focal choroidal granuloma is seen as a localized elevation and thickening of the choroid

with possible subretinal fluid (Goldberg and Jabs 2015; Saxena et al. 2013) (Fig. 25.23). Within the subretinal fluid area, there may be a point of adhesion between the neurosensory retina and RPE-Bruch's membrane with the overlying hyper-reflective retina (Salman et al. 2006) (Figs. 25.24 and 25.25).

B. Tuberculous serpiginous-like choroiditis (TB-SLC)

TB-SLC starts as unilateral, multifocal lesions that coalesce and involve the periphery (Vasconcelos-Santos et al. 2010) in comparison to the bilateral, disc centric lesions of classic serpiginous choroiditis (SC).

OCT imaging in TB-SLC is similar to classic SC. Active lesions show hyper-reflective and blurred outer retinal layers and RPE. There may be some elevation of the retina and RPE

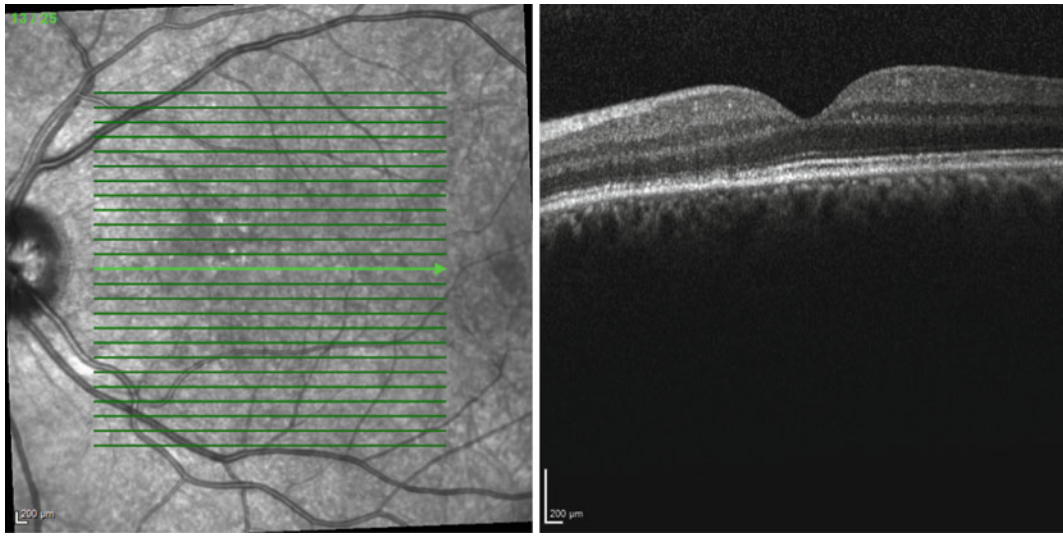

Fig. 25.22 Acute syphilitic posterior placoid chorioretinitis. SD-OCT 1 month after intravenous penicillin with almost complete reformation of the outer retinal lamellae

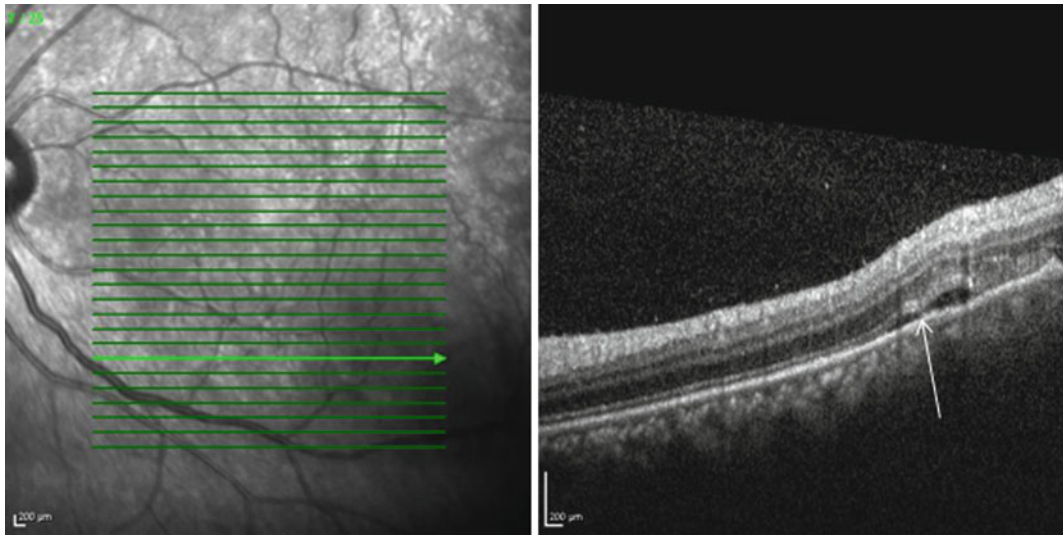

Fig. 25.23 Tuberculous chorioretinitis. SD-OCT showing a case of possible tuberculous choroidal granuloma. Evidence of subretinal fluid with an area of adhesion between the retina and RPE-Bruch's membrane (*white arrow*)

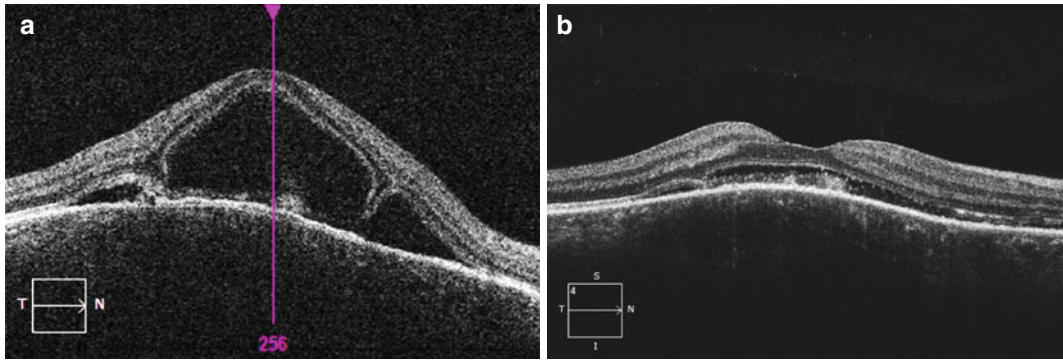

Fig. 25.24 Tubercular choroidal granuloma. (**a**) Pretreatment. SD-OCT showing elevated choroid with associated subretinal fluid and adhesion between the neurosensory retina and RPE-Bruch's membrane. (**b**) Post-antitubercular treatment. Significant reduction of both choroidal elevation and reduction in subretinal fluid with antitubercular treatment

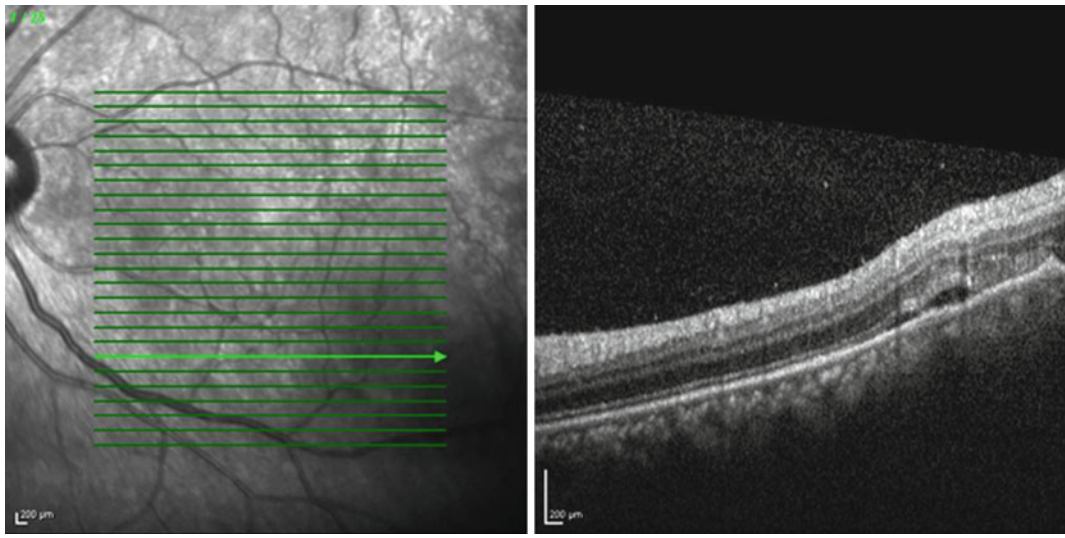

Fig. 25.25 Tuberculous choroidal granuloma. SD-OCT showing subretinal fluid with an area of adhesion between the retina and RPE-Bruch's membrane

by the underlying choroid (Rifkin et al.). As the lesions heal, the outer retina displays irregular lumpy elevations that progresses to atrophy of the outer retina, RPE and choroid (Bansal et al. 2011; Rifkin et al. 2015).

25.4.1.3 *Bartonella henselae* Neuroretinitis

Also called cat scratch disease (CSD), this condition is manifested clinically by optic nerve swelling with the appearance of a macular star of exudate. In the acute phase, OCT demonstrates outer plexiform cystic oedema emanating from the disc and macular serous detachment (Habot-Wilner et al. 2011; Stewart et al. 2005). As the fluid is reabsorbed in the convalescent phase, the lipid precipitates in the outer plexiform layer to form a macular star. The precipitates are seen as hyper-reflective elements in the outer plexiform layer (Habot-Wilner et al. 2011).

25.4.2 Viral Posterior Uveitis

25.4.2.1 Herpes Retinitis

Herpes simplex virus (HSV), herpes zoster virus and cytomegalovirus (CMV) are potential causes of infectious necrotizing retinitis. This may be manifested as various clinical syndromes including acute retinal necrosis (ARN) and progressive outer retinal necrosis (PORN). Most reports on OCT imaging relate to PORN and CMV retinitis because of difficulty obtaining quality OCT images of the peripheral retina and the presence of dense vitritis. Retinitis due to these herpes viruses all appears similar on OCT imaging in the acute phase. At presentation of an acute lesion with active white retinal necrosis, the OCT demonstrates outer retinal oedema and inner retinal hyper-reflectivity (Arichkia et al. 2016; Blair et al. 2007; Narayanan and Kuppermann 2006; Yeh et al. 2010) (Fig. 25.26). Over weeks to months with antiviral treatment, the retina undergoes cystic oedema and subsequent profound atrophy (Blair et al. 2007; Sun et al. 2012; Yeh et al. 2010). Due to the slower nature of CMV retinitis, the OCT images may display partial atrophy and inflammation simultaneously. Figure 25.27 shows a resolved CMV retinitis.

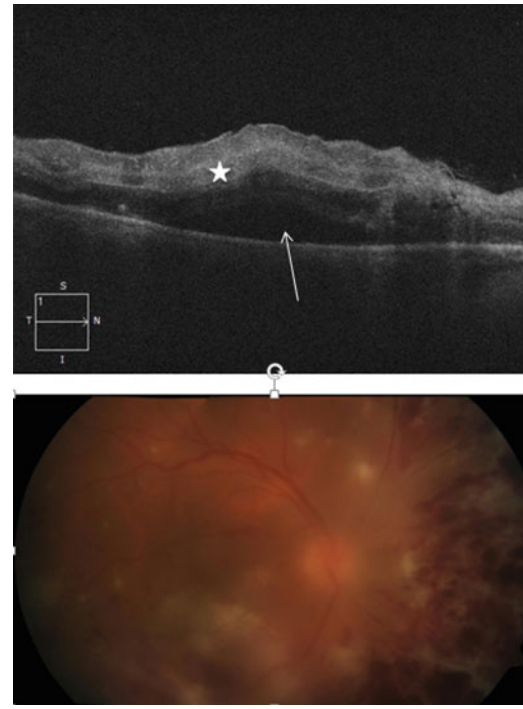

Fig. 25.26 Varicella zoster virus-related acute retinal necrosis (ARN). SD-OCT of the macula showing severe retinal thickening, inner retinal hyper-reflectivity (*white star*) and disruption of outer retinal layers with associated subretinal fluid (*white arrow*). Corresponding colour photo of the fundus showing vitreous haze, diffuse retinal oedema associated with scattered exudates and haemorrhages

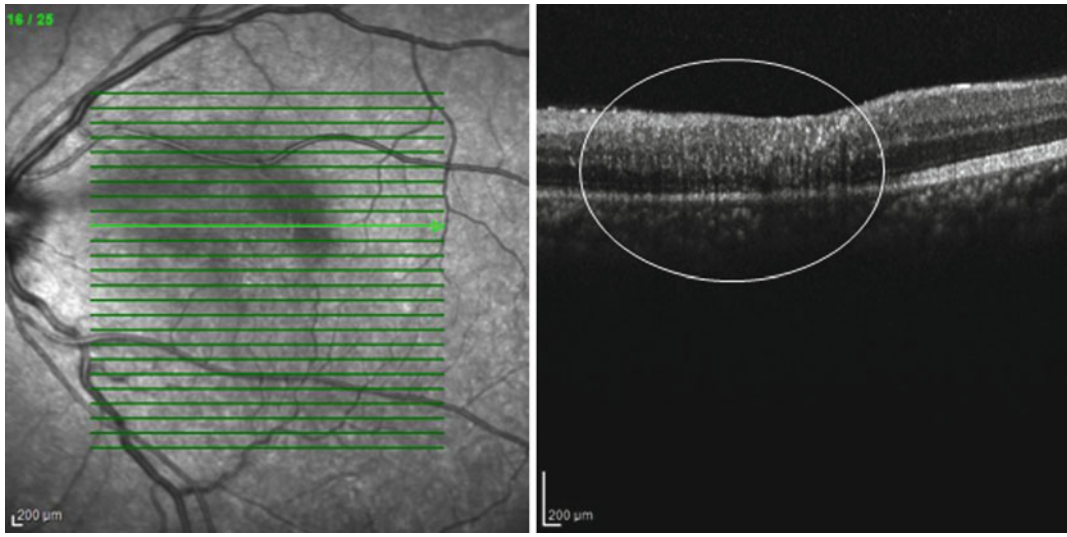

Fig. 25.27 Cytomegalovirus-related retinitis. SD-OCT shows full-thickness loss of the lamellar retinal structure, hyper-reflective inner retina and partial retinal thinning developing suggesting chronicity (*white circle*)

25.4.2.2 Coxsackie Virus Maculopathy

Also known as unilateral acute idiopathic maculopathy (UAIM), this condition has a strong association with coxsackievirus infection (Beck et al. 2004). Acute infection is seen as subfoveal neurosensory retinal detachment with hyper-reflective debris on the apical side of the RPE, possibly representing photoreceptor outer segments (Jung et al. 2012). During convalescence, the neurosensory detachment resolves, and the outer retinal layers appear disrupted (Jung et al. 2012).

In the resolved phase, there is almost complete restoration of foveal anatomy but with some residual disruption of the EZ (Srour et al. 2013). The RPE may appear slightly elevated and thickened (Srour et al. 2013).

25.4.2.3 Dengue Maculopathy

Dengue fever can cause ocular complications in up to 10 % of patients (Su et al. 2007). Acute macular findings in such cases can include diffuse retinal thickening, cystoid macular oedema or a foveolitis seen as thickening and high reflectivity of the outer retina (Teoh et al. 2010) (Fig. 25.28). Return to normal anatomy occurs over 1 month, but up to 60 % have persistent paracentral scotomas at 2 years (Teoh et al. 2010).

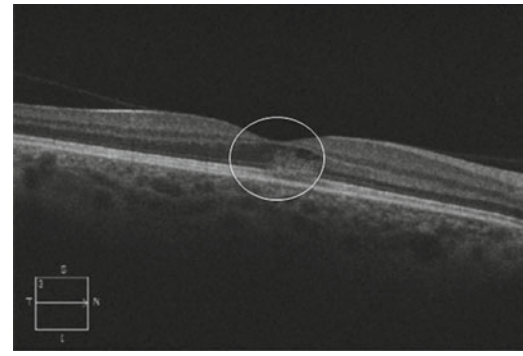

Fig. 25.28 Dengue maculopathy. SD-OCT shows 'foveolitis' and mild cystic oedema (*white circle*)

25.4.3 Fungal Posterior Uveitis

25.4.3.1 Candida Chorioretinitis

Ocular candidiasis may present with predominantly vitreal pathology with or without chorioretinal lesions. In cases with chorioretinal abscesses, early or small lesions show protrusion of material at the level of the RPE into the outer retina. More significant lesions may demonstrate a hyper-reflective, elevated lesion protruding into the vitreoretinal interface with significant shadowing of the underlying layers (Cho et al. 2007). Elevation of the adjacent RPE suggests a choroidal origin (Lavine and Mititelu 2015). In the resolved state, smaller lesions gradually regress with reformation of the external limiting membrane but with residual RPE irregularity (Cho et al. 2007). The more advanced lesions also regress with flattening of the vitreoretinal protrusion, and the affected retina is replaced by a full-thickness hyper-reflectivity indicative of scar formation (Lavine and Mititelu 2015).

25.4.4 Parasitic Posterior Uveitis

25.4.4.1 Toxoplasmic Retinochoroiditis

Acute toxoplasmosis infection by replicating tachyzoites may produce two clinical manifestations: classic toxoplasmic retinochoroiditis and punctate outer retinal toxoplasmosis (PORT).

A. Classic retinal toxoplasmosis
   Acute retinal infection will be represented on OCT as thickening, hyper-reflectivity and disruption of the entire neurosensory retina that gives a 'smudge'-like appearance (Fig. 25.29) (Goldenberg et al. 2013; Oréfice et al. 2006). The full-thickness involvement of the retina helps distinguish toxoplasmic retinal infection from a cotton wool spot that shows relative sparing of the outer retina (Kurup et al. 2014). Other findings include possible subretinal fluid (Diniz et al. 2011) and thickening of the posterior hyaloid with partial detachment over the lesion (Goldenberg et al. 2013). The underlying choroid is significantly thickened on enhanced depth imaging optical coherence tomography (EDI-OCT) scans, and this returns to normal during resolution (Goldenberg et al. 2013). In some eyes, hyper-reflective spherical deposits may be detected at the vitreoretinal interface.

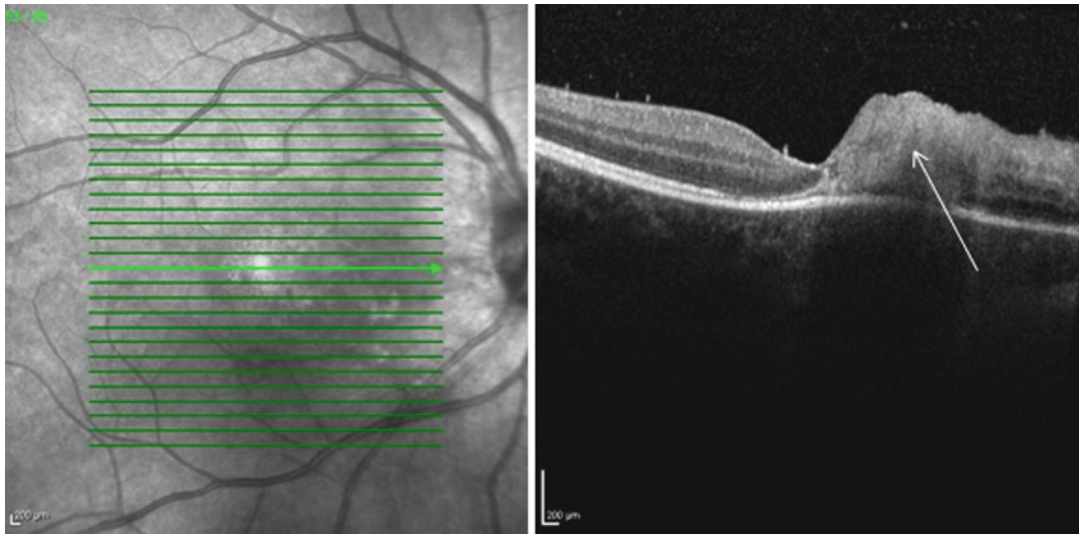

Fig. 25.29 Toxoplasmic retinochoroiditis. SD-OCT shows full-thickness involvement of neurosensory retina with a 'smudge-like' appearance in the acute phase (*white arrow*) and vitreal cells

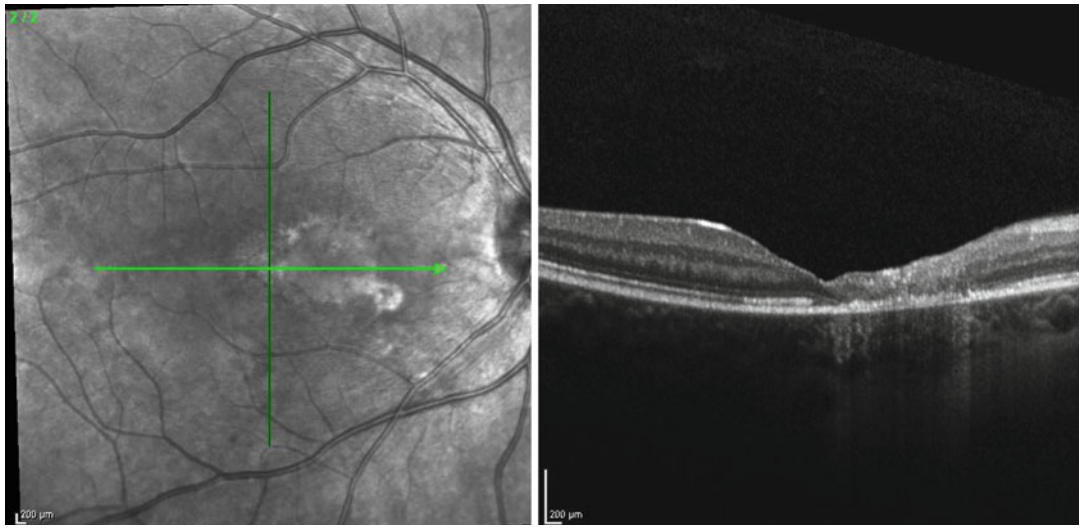

Fig. 25.30 Toxoplasmic retinochoroiditis. SD-OCT, 3 weeks after initial presentation and with treatment, shows full-thickness retinal disorganization and atrophy on the nasal side of the fovea

These may be remote from the infective focus and may occur along retinal vessels (Guagnini et al. 2007; Oréfice et al. 2013). As the lesion heals, these deposits may be incorporated into the inner retina and then dissolved (Goldenberg et al. 2013).

B. Punctate outer retinal toxoplasmosis (PORT)
Acute infection of the outer retina and RPE appears as hyper-reflectivity of the inner retina with shadowing of the outer retina and a focally detached posterior hyaloid face (Oréfice et al. 2007). There may also be subretinal fluid accumulation and fluid accumulation in the outer retina in a cystic-like appearance (Lujan 2014).

For both subtypes, as the lesion heals, there is further separation of the hyaloid, epiretinal membrane formation, retinal thinning and permanent loss and disorganization of the outer retinal elements (Fig. 25.30) (Diniz et al. 2011;

Oréfice et al. 2006). The residual scar may demonstrate various appearances including retinal atrophy and disorganization with thinning, an elevated retinal scar, deep (outer) retinal scar with excavation or a combination of these patterns (Goldenberg et al. 2013). Some patients may develop vitreomacular traction (Oréfice et al. 2006) or potential full-thickness macular hole (Panos et al. 2013).

25.4.4.2 Other Parasitic Infections

A. *Toxocara*

Acute *Toxocara* infection has been imaged as a mobile hyper-reflectivity on the inner retinal surface protruding into the vitreous (Sukuzi et al. 2005; Hashida et al. 2014). A significant granulomatous retinal reaction can occur and appears as hyper-reflectivity in the subretinal space or on the retinal surface (Shimzu et al. 2005). A tractional retinal fold emanating from the granuloma may be observed and on OCT appears as a diffusely hyper-reflective area of the elevated retina and surrounding subretinal fluid (Verallo et al. 2012; Shimzu et al. 2005).

B. Diffuse unilateral subacute neuroretinitis (DUSN)

This is a clinical presentation of unilateral retinal wipeout due to a retinal worm infection. OCT in late-phase disease demonstrates predominantly inner retinal thinning with loss of retinal nerve fibre layer (Garcia Filho et al. 2012). On OCT the worm may appear as a hyper-reflective outer retinal structure with surrounding disturbance of retinal lamellae (Garcia Filho et al. 2012). Another case has shown the worm residing on the retinal surface (Cunha et al. 2010).

25.5 Haemorrhagic Occlusive Retinal Vasculitis (HORV)

A recently described entity, haemorrhagic occlusive retinal vasculitis (HORV), occurs postoperatively and is associated with intraocular use of vancomycin (Witkin et al. 2015). Clinically, the condition may mimic viral retinitis, postoperative endophthalmitis or toxic anterior segment syndrome. The difference is the relative lack of pain and anterior segment inflammation in the presence of severe retinal changes. Prognostically, these patients have very poor visual outcome and often are complicated with neovascular glaucoma. Early OCT changes may show serous retinal detachment, disruption of the outer retinal layers and increased macular oedema with hyper-reflective inner retina (Witkin et al. 2015) (Fig. 25.31). Later OCT may show resolution of retinal oedema and hyper-reflectivity. Hyper-reflective lesions representing

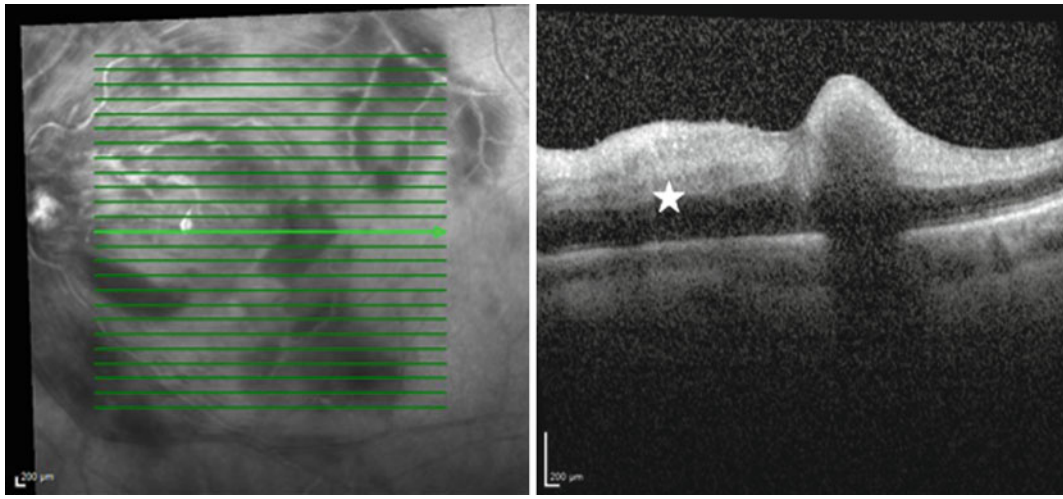

Fig. 25.31 Haemorrhagic occlusive retinal vasculitis (HORV). SD-OCT with corresponding red-free showing thickening of all retinal layers with hyper-reflectivity of the inner retinal layers (*white star*) suggesting retinal ischaemia

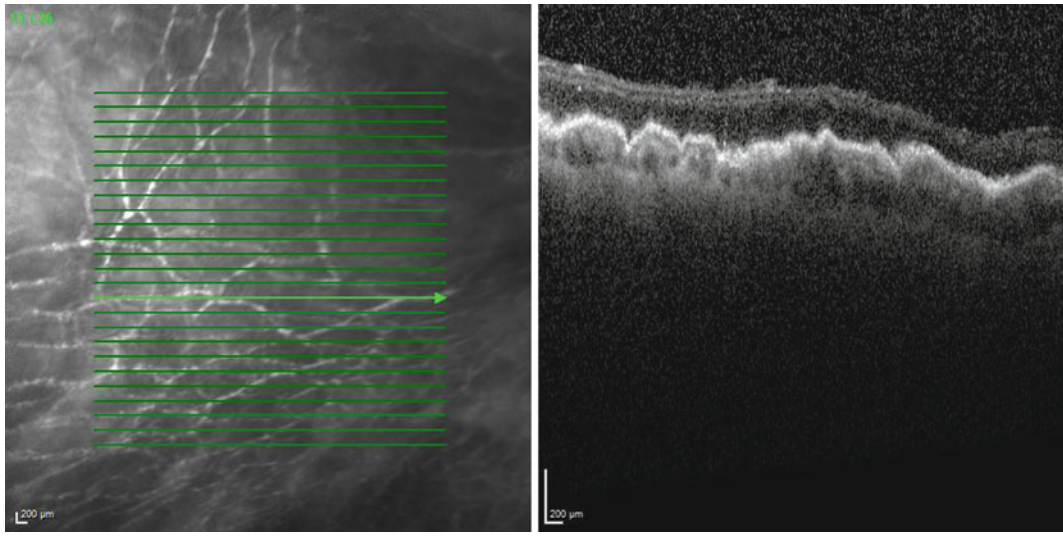

Fig. 25.32 Haemorrhagic occlusive retinal vasculitis. SD-OCT of the right eye 6 months following HORV shows severe retinal thinning of all layers with loss of outer retinal layers. Note hyper-reflective spot in the outer plexiform layer representing hard exudate

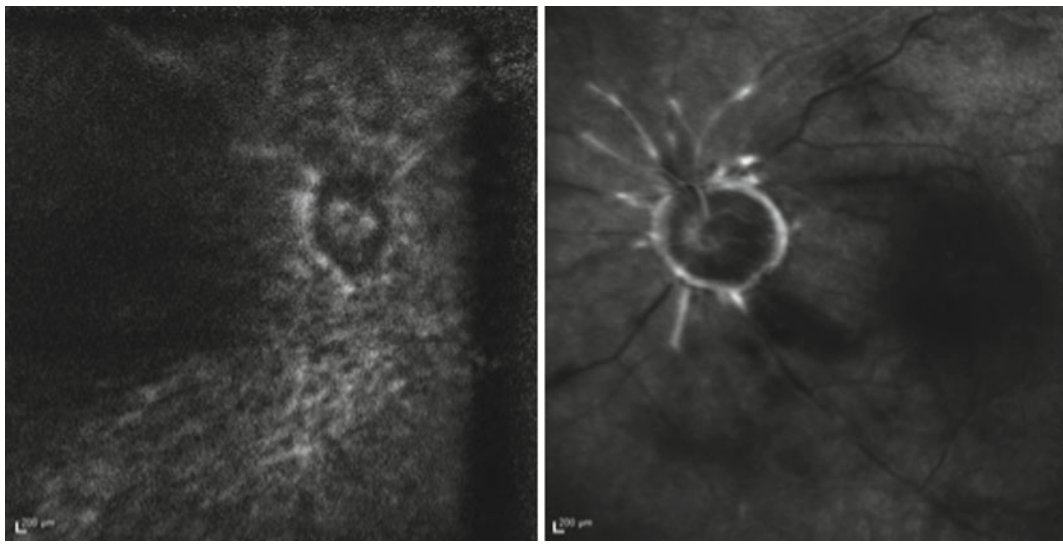

Fig. 25.33 Haemorrhagic occlusive retinal vasculitis. Corresponding FFA of both the left and right eye with HORV. The right showing complete non-perfusion of retinal circulation 6 months following HORV, whilst the left showing staining of retinal vessels with minimal perfusion beyond 1 disc diameter from the disc

hard exudates in the outer plexiform layer may persist (Witkin et al. 2015). Months after onset, OCT may show diffuse atrophy of all retinal layers and loss of outer retinal layers (Figs. 25.32 and 25.33).

25.6 Posterior Scleritis

Posterior scleritis is a specific form of scleral inflammation with very variable clinical presentation. Up to one third of patients with posterior

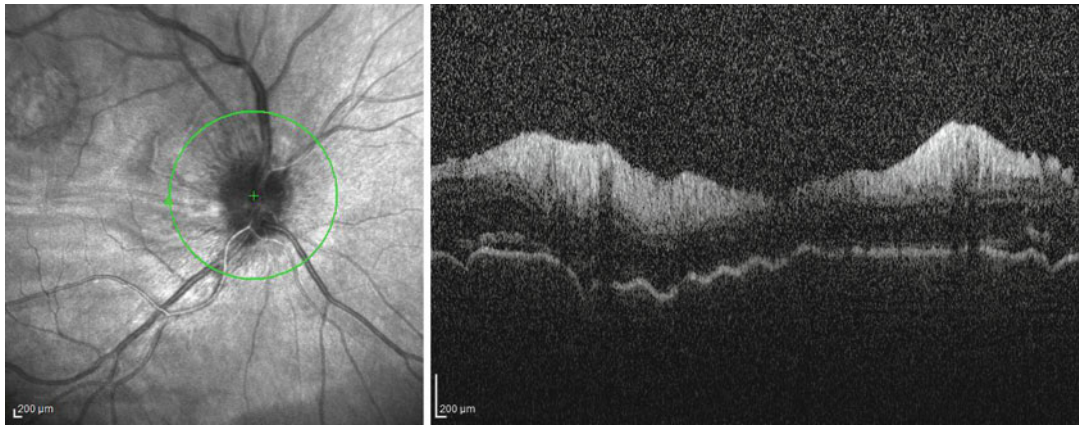

Fig. 25.34 Posterior scleritis. SD-OCT showing swollen optic disc associated with nodular posterior scleritis

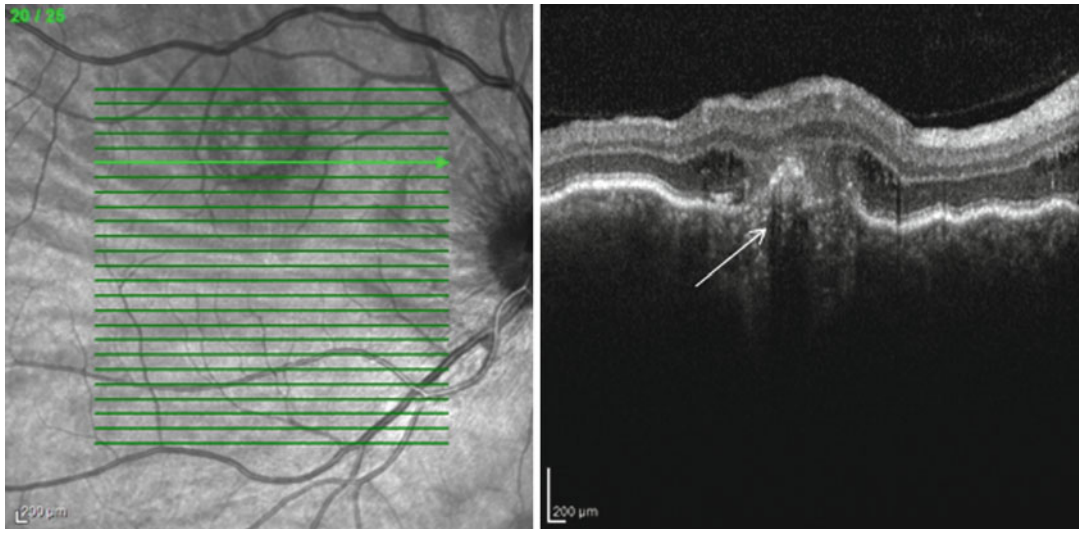

Fig. 25.35 Posterior scleritis. SD-OCT of the right optic nerve showing disc swelling associated with nodular posterior scleritis (*visible on red-free*). SD-OCT raster over the lesion showing focal choroidal elevation (*white arrow*) and intra-retinal fluid

scleritis have systemic association such as rheumatoid arthritis, granulomatosis with polyangiitis, relapsing polychondritis, etc. Clinical features of posterior scleritis are characterized most frequently by serous retinal detachment, swollen optic disc (Fig. 25.34), localized subretinal granuloma and uveitis. Nodular posterior scleritis presents as nodular subretinal mass which can be imaged on OCT (Fig. 25.35). This can be associated with retinal pigment epithelial changes, subretinal fluid, macular oedema and choroidal folds (Agrawal et al. 2016). OCT findings in scleritis are typically nonspecific, and other imaging modalities, e.g. ultrasound and CT, are used to show focal choroidal thickening. Studies reporting on OCT features in posterior scleritis are rare. OCT may show choroidal thickening with associated cystic subretinal spaces which typically resolves with treatment (Erdol et al. 2008).

25.7 Masquerade Syndromes

25.7.1 Intraocular Lymphoma

Primary CNS lymphoma is an important differential for panuveitis. Whilst confirmatory testing will require vitreous biopsy or lumbar puncture, various authors have described longitudinal OCT features that may point to a diagnosis of PCNSL (Liu et al. 2012). Early OCT may show hyper-reflective material within the outer retina that obscures EZ and ELM and increased irregularity in the RPE (Fig. 25.36). This is associated with disruption to the outer nuclear layer and outer plexiform layer (Liu et al. 2012). Later OCTs may show RPE elevation accompanied by heterogeneous, hyper-reflective sub-RPE deposits. Importantly, retinal and subretinal deposits may resolve with treatment-making OCT a useful modality to monitor treatment response (Forooghian et al. 2011) (Fig. 25.37).

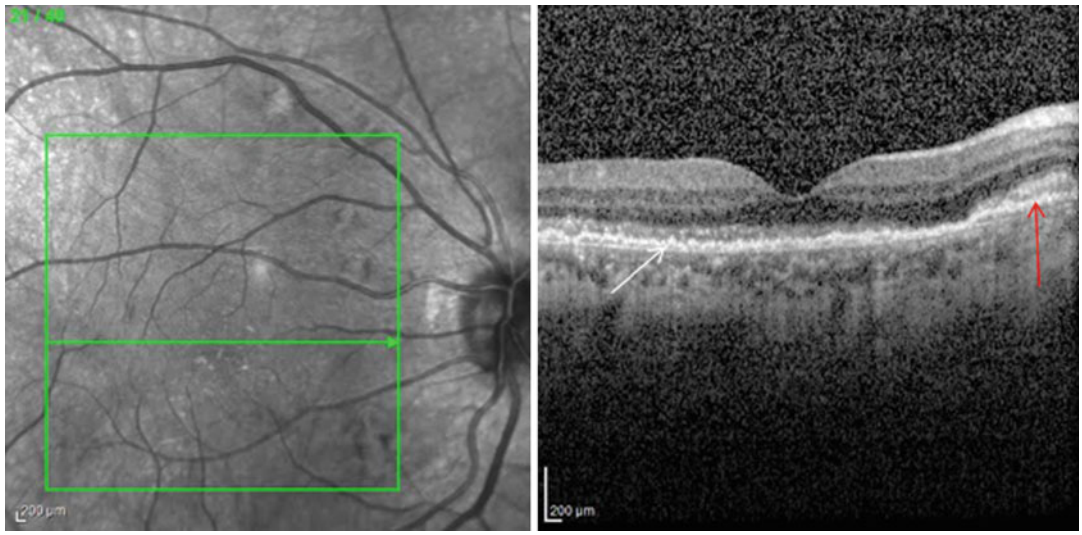

Fig. 25.36 Intraocular lymphoma. Pretreatment SD-OCT showing hyper-reflectivity above the RPE (*red arrow*) with loss of EZ and ELM. Note also the increase irregularity of RPE temporally (*white arrow*)

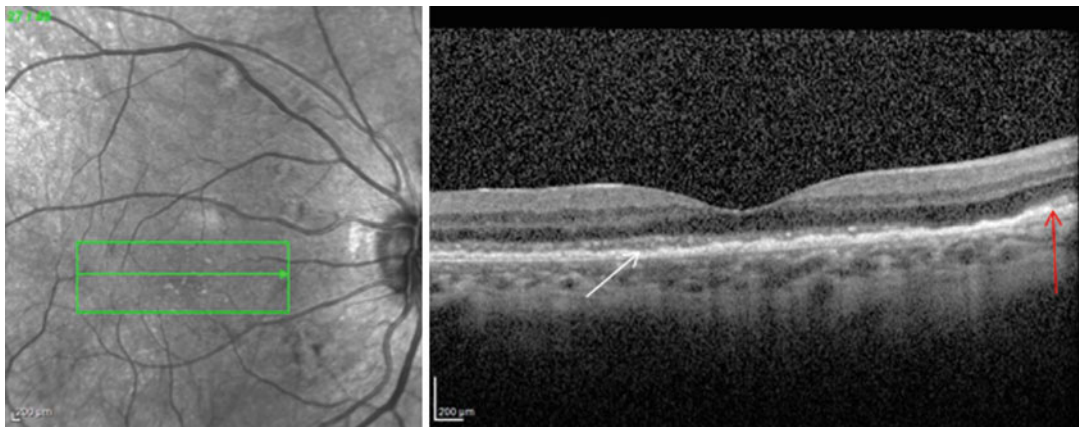

Fig. 25.37 Intraocular lymphoma. Posttreatment SD-OCT showing reduction in hyper-reflectivity deposit above RPE (*red arrow*) and significant reduction in RPE irregularity (*white arrow*)

References

Agrawal R, Lavric A, Restori M, Pavesio C, Sagoo MS (2016) NODULAR POSTERIOR SCLERITIS: clinico-sonographic characteristics and proposed diagnostic criteria. Retina 36(2):392–401

Amer R, Florescu T (2008) Optical coherence tomography in relentless placoid chorioretinitis. Clin Experiment Ophthalmol 36:388–390. doi:10.1111/j.1442-9071.2008.01773.x

Amin HI (2006) Optical coherence tomography findings in multiple evanescent white dot syndrome. Retina 26:483–484

Arantes TEF, Matos K, Garcia CR et al (2011) Fundus autofluorescence and spectral domain optical coherence tomography in recurrent serpiginous choroiditis: case report. Ocul Immunol Inflamm 19:39–41

Arichkia S, Uji A, Yoshimura N (2016) Retinal structural features of cytomegalovirus retinitis with acquired immunodeficiency syndrome: an adaptive optics imaging and optical coherence tomography study. Clin Experiment Ophthalmol 44(1):62–64. doi:10.1111/ceo.12577

Bansal R, Kulkarni P, Gupta A (2011) High-resolution spectral domain optical coherence tomography and fundus autofluorescence correlation in tubercular serpiginous like choroiditis. J Ophhtalmic Inflamm Infect 1:157–163

Beck AP, Jampol LM, Glaser DA et al (2004) Is coxsackie virus the cause of unilateral acute idiopathic maculopathy? Arch Ophthalmol 122:121–123

Birnbaum AD, Blair MP, Tessler HH et al (2010) Subretinal fluid in acute posterior multifocal placoid pigment epitheliopathy. Retina 30:810–814

Birnbaum AD, Fawzi AA, Rademaker A et al (2014) Correlation between clinical signs and optical coherence tomography with enhanced depth imaging findings in patients with birdshot chorioretinopathy. JAMA Ophthalmol 132:929–935

Blair MP, Goldstein DA, Shapiro MJ (2007) Optical coherence tomography of progressive outer retinal necrosis. Retina 27:1313–1314

Brito P, Penas S, Carneiro Â et al (2011) Spectral-domain optical coherence tomography features of acute syphilitic posterior placoid chorioretinitis: the role of autoimmune response in pathogenesis. Case Rep Ophthalmol 2:39–44

Channa R, Ibrahim M, Sepah Y et al (2012) Characterization of macular lesions in punctate inner choroidopathy with spectral domain optical coherence tomography. J Ophthalmic Inflamm Infect 2:113–120

Chen X, Rahimy E, Sergott RC et al (2015) Spectrum of retinal vascular diseases associated with paracentral acute middle maculopathy. Am J Ophthalmol 160: 26–34

Cho M, Khanifar AA, Chan RV (2007) Spectral-domain optical coherence tomography of endogenous fungal endophthalmitis. Retina Cases Brief Rep 5:136–140

Cunha LP, Costa-Cunha LV, Souza EC et al (2010) Intraretinal worm documented by optical Coherence tomography in a patient with diffuse unilateral subacute neuroretinitis: case report. Arq Bras Oftalmol 73:462–463

da Silva FT, Sakata VM, Nakashima A et al (2013) Enhanced depth imaging optical coherence tomography in long-standing Vogt-Koyanagi-Harada disease. Br J Ophthalmol 91:70–74

de Bats F, Wolff B et al (2014) "En-Face" spectral-domain optical coherence tomography findings in multiple evanescent white dot syndrome. J Ophthalmol 2014:928028. doi:10.1155/2014/928028

de Smet MD, Rao NA (2005) Retinal cystoid spaces in acute Vogt-Koyanagi-Harada syndrome. Am J Ophthalmol 140:962

Diniz B, Regatieri C, Andrade R et al (2011) Evaluation of spectral domain and time domain optical coherence tomography findings in toxoplasmic retinochoroiditis. Clin Ophthalmol 5:645–650

Dolz-Marco R, Rodríguez-Ratón A, Hernández-Martínez P, Pascual-Camps I, Andreu-Fenoll M, Gallego-Pinazo R (2014) Macular retinal and choroidal thickness in unilateral relentless placoid chorioretinitis analyzed by swept-source optical coherence tomography. J Ophthalmic Inflamm Infect 4:24. doi:10.1186/s12348-014-0024-x

Erdol H, Kola M, Turk A (2008) Optical coherence tomography findings in a child with posterior scleritis. Eur J Ophthalmol 18:1007–1010

Fawzi AA, Pappuru RR, Sarraf D et al (2012) Acute macular neuroretinopathy: long-term insights revealed by multimodal imaging. Retina 32:1500–1513

Feigl B, Haas A (2000) Optical Coherence Tomography (OCT) in acute macular neuroretinopathy. Acta Ophthalmol Scand 78:714–716

Fong AH, Li KK, Wong D (2011) Choroidal evaluation using enhanced depth imaging spectral-domain optical coherence tomography in Vogt-Koyanagi-Harada disease. Retina 31:502–509

Forooghian F, Yeh S, Faia LJ, Nussenblatt RB (2009) Uveitic foveal atrophy: clinical features and associations. Arch Ophthalmol 127:179–186, doi:10.1001

Forooghian F, Merkur AB, White VA, Shen D, Chan CC (2011) High-definition optical coherence tomography features of primary vitreoretinal lymphoma. Ophthalmic Surg Lasers Imaging 42 Online:e97–e99. doi:10.3928/15428877-20110922-02

Fujiwara T, Imamura Y, Giovinazzo VJ et al (2010) Fundus autofluorescence and optical coherence tomographic findings in acute zonal occult outer retinopathy. Retina 30:1206–1216

Garcia Filho CA, Garcia CA, Arevalo JF (2012) Imaging in the diagnosis and management of diffuse unilateral subacute neuroretinitis. Int Ophthalmol Clin 52:283–289

Goldberg NR, Jabs DA (2015) Multimodal imaging of a tuberculous granuloma. Retina 35:1919–1920

Goldberg NR, Jabs DA, Busingye J (2015) Optical coherence tomography imaging of presumed sarcoid retinal and optic nerve nodules. Ocul Immunol Inflamm 24:1–4

Goldenberg D, Goldstein M, Loewenstein A et al (2013) Vitreal, retinal, and choroidal findings in active and

scarred toxoplasmosis lesions: a prospective study by spectral-domain optical coherence tomography. Graefes Arch Clin Exp Ophthalmol 251:2037–2045

Guagnini AP, De Potter P, Levecq L et al (2007) Atypical spherical deposition on vitreoretinal interface associated with toxoplasmic chorioretinitis. Graefes Arch Clin Exp Ophthalmol 245:158–160

Gupta V, Gupta A, Gupta P et al (2009) Spectral-domain cirrus optical coherence tomography of choroidal striations seen in the acute stage of Vogt-Koyanagi-Harada disease. Am J Ophthalmol 147:148–153

Habot-Wilner Z, Zur D, Goldstein M et al (2011) Macular findings on optical coherence tomography in cat-scratch disease neuroretinitis. Eye (Lond) 25:1064–1068

Hashida N, Nakai K, Nishida K (2014) Diagnostic evaluation of ocular toxocariasis using high-penetration optical coherence tomography. Case Rep Ophthalmol 5:16–21

Hashimoto H, Kishi S (2015) Ultra-wide-field fundus autofluorescence in multiple evanescent white dot syndrome. Am J Ophthalmol 159:698–706

Hughes EG, Siow YC, Hunyor AP (2009) Acute macular neuroretinopathy: anatomic localization of the lesion with high-resolution OCT. Eye (Lond) 23: 2132–2134

Invernizzi A, Mapelli C, Viola F et al (2015) Choroidal granulomas visualized by enhanced depth imaging optical coherence tomography. Retina 35:525–531

Ishihara K, Hangai M, Kita M et al (2009) Acute Vogt-Koyanagi-Harada disease in enhanced spectral-domain optical coherence tomography. Ophthalmology 116:1799–1807

Joseph A, Rogers S, Browning A et al (2007) Syphilitic acute posterior placoid chorioretinitis in nonimmunocompromised patients. Eye (Lond) 21:1114–1119

Jung CS, Payne JF, Bergstrom CS (2012) Multimodality diagnostic imaging in acute idiopathic maculopathy. Arch Ophthalmol 130:50–56

Kanis MJ, van Norren D (2006) Integrity of foveal cones in multiple evanescent white dot syndrome assessed with OCT and foveal reflection analyser. Br J Ophthalmol 90:795–796

Keane PA, Allie M, Turner SJ et al (2013) Characterization of birdshot chorioretinopathy using extramacular enhanced depth optical coherence tomography. JAMA Ophthalmol 131:341–350

Kurup SP, Khan S, Gill MK (2014) Spectral domain optical coherence tomography in the evaluation and management of infectious retinitis. Retina 34:2233–2241

Lavine JA, Mititelu M (2015) Multimodal imaging of refractory Candida chorioretinitis progressing to endogenous endophthalmitis. J Ophthalmic Inflamm Infect 5:54

Lee GE, Lee BW, Rao NA et al (2011) Spectral domain optical coherence tomography and autofluorescence in a case of acute posterior multifocal placoid pigment epitheliopathy mimicking Vogt-Koyanagi-Harada disease: case report and review of the literature. Ocul Immunol Inflamm 19:42–47

Li D, Kishi S (2007) Loss of photoreceptor outer segment in acute zonal occult outer retinopathy. Arch Ophthalmol 125:1194–2000

Li D, Kishi S (2009) Restored photoreceptor outer segment damage in multiple evanescent white dot syndrome. Ophthalmology 116:763–770

Lim LL, Watzke RC, Lauer AK et al (2006) Ocular coherence tomography in acute posterior multifocal placoid pigment epitheliopathy. Clin Experiment Ophthalmol 34:810–812

Liu TY, Ibrahim M, Bittencourt M, Sepah YJ, Do DV, Nguyen QD (2012) Retinal optical coherence tomography manifestations of intraocular lymphoma. J Ophthalmic Inflamm Infect 2:215–218

Lujan BJ (2014) Spectral domain optical coherence tomography imaging of punctate outer retinal toxoplasmosis. Saudi J Ophthalmol 28:152–156

Markomichelakis NN, Halkiadakis I, Pantelia E et al (2004) Patterns of macular edema in patients with uveitis: qualitative and quantitative assessment using optical coherence tomography. Ophthalmology 111: 946–953

Maruko I, Iida T, Sugano Y et al (2011) Subfoveal choroidal thickness after treatment of Vogt-Koyanagi-Harada disease. Retina 31:510–517

Modi YS, Epstein A, Bhaleeya S et al (2013) Multimodal imaging of sarcoid choroidal granulomas. J Ophthalmic Inflamm Infect 3:58

Monnet D, Levinson RD, Holland GN (2007) Longitudinal cohort study of patients with birdshot chorioretinopathy. III. Macular imaging at baseline. Am J Ophthalmol 144:818–828

Monson BK, Greenberg PB, Greenberg E et al (2007) High-speed, ultra-high-resolution optical coherence tomography of acute macular neuroretinopathy. Br J Ophthalmol 91:119–120

Montero JA, Ruiz-Moreno JM, Fernandez-Munoz M (2011) Spectral domain optical coherence tomography findings in acute posterior multifocal placoid pigment epitheliopathy. Ocul Immunol Inflamm 19:48–50

Mrejen S, Khan S, Gallego-Pinazo R et al (2014) Acute zonal occult outer retinopathy: a classification based on multimodal imaging. JAMA Ophthalmol 132: 1089–1098

Narayanan R, Kuppermann BD (2006) Optical coherence tomography in progressive outer retinal necrosis. Ophthalmic Surg Lasers Imaging 37:506–507

Oréfice JL, Cost RA, Campos W et al (2006) Third-generation optical coherence tomography findings in punctate retinal toxoplasmosis. Am J Ophthalmol 142:503–505

Oréfice JL, Costa RA, Oréfice F et al (2007) Vitreoretinal morphology in active ocular toxoplasmosis: a prospective study by optical coherence tomography. Br J Ophthalmol 91:773–780

Oréfice JL, Cost RA, Scott IU et al (2013) Spectral optical coherence tomography findings in patients with ocular toxoplasmosis and active satellite lesions (MINAS Report 1). Acta Ophthalmol 91:e41–e47

Panos GD, Papageorgiou E, Kozeis N et al (2013) Macular hole formation after toxoplasmic retinochoroiditis. BMJ Case Rep bcr2013008915

Pichi F, Ciardella AP, Cunningham ET Jr et al (2014) Spectral domain optical coherence tomography findings in patients with acute syphilitic posterior placoid chorioretinopathy. Retina 34:373–384

Punjabi OS, Rich R, Davis JL et al (2008) Imaging serpiginous choroidopathy with spectral domain optical coherence tomography. Ophthalmic Surg Lasers Imaging 39:S95–S98

Rahimy E, Sarraf D, Dollin ML et al (2014) Paracentral acute middle maculopathy in nonischemic central retinal vein occlusion. Am J Ophthalmol 158:472–480

Reynard M, Riffenburgh RS, Minckler DS (1985) Morphological variation of Dalén-Fuchs nodules in sympathetic ophthalmia. Br J Ophthalmol 69: 197–201

Rifkin LM, Munk MR, Baddar D et al (2015) A new finding in tuberculous serpiginous-like choroidopathy. Ocul Immunol Inflamm 23:53–58

Rostaqui O, Querques G, Haymann P et al (2014) Visualization of sarcoid choroidal granuloma by enhanced depth imaging optical coherence tomography. Ocul Immunol Inflamm 22:239–241

Salman A, Parmar P, Rajamohan M et al (2006) Optical coherence tomography in choroidal tuberculosis. Am J Ophthalmol 142:170–172

Sarraf D, Rahimy E, Fawzi AA et al (2013) Paracentral acute middle maculopathy: a new variant of acute macular neuroretinopathy associated with retinal capillary ischemia. JAMA Ophthalmol 131:1275–1287

Saxena S, Singhal V, Ajduman L (2013) Three-dimensional spectral domain optical coherence tomography imaging of the retina in choroidal tuberculoma. BMJ Case Rep 2013. bcr2012008156

Scheufele TA, Witkin AJ, Schocket LS et al (2005) Photoreceptor atrophy in acute posterior multifocal placoid pigment epitheliopathy demonstrated by optical coherence tomography. Retina 25:1109–1112

Shimzu Y, Imai M, Fukasawa A et al (2005) Premacular membrane peeling without removal of subretinal granuloma in an eye with ocular toxocariasis. Acta Ophthalmol Scand 83:395–396

Souka AAR, Hillenkamp J, Gora F et al (2006) Correlation between optical coherence tomography and autofluorescence in acute posterior multifocal placoid pigment epitheliopathy. Graefes Arch Clin Exp Ophthalmol 244:1219–1223

Spaide RF, Koizumi H, Freund KB (2008) Photoreceptor outer segment abnormalities as a cause of blind spot enlargement in acute zonal occult outer retinopathy-complex diseases. Am J Ophthalmol 146:111–120

Spaide RF, Goldberg N, Freund KB (2013) Redefining multifocal choroiditis and panuveitis and punctate inner choroidopathy through multimodal imaging. Retina 33:1315–1324

Srour M, Querques G, Rostaqui O et al (2013) Early spectral-domain optical coherence tomography findings in unilateral acute idiopathic maculopathy. Retina 33:2182–2184

Staurenghi G, Sadda S, Chakravarthy U, Spaide RF (2014) International Nomenclature for Optical Coherence Tomography (IN•OCT) Panel. Proposed lexicon for anatomic landmarks in normal posterior segment spectral-domain optical coherence tomography: the IN•OCT consensus. Ophthalmology 121:1572–1578. doi:10.1016/j.ophtha.2014.02.023

Stewart MW, Brazis Paul W, Barrett KM et al (2005) Optical coherence tomography in a case of bilateral neuroretinitis. J Neuro Ophthalmol 25:131–133

Su DH, Bascl K, Chee SP et al (2007) Prevalence of dengue maculopathy in patients hospitalized for dengue fever. Ophthalmology 114:1743–1747

Sukuzi T, Joko T, Akao N et al (2005) Following the migration of a Toxocara lava in the retina by optical coherence tomography and fluorescein angiography. Jpn J Ophthalmol 49:159–161

Sun LL, Goodwin T, Park JJ (2012) Optical coherence tomography changes in macular CMV retinitis. Digit J Ophthalmol 18:1–4

Teoh SC, Chee CK, Laude A et al (2010) Optical coherence tomography patterns as predictors of visual outcome in dengue-related maculopathy. Retina 30:390–398

Tsjuikawa A, Yamashiro K, Yamamoto K et al (2005) Retinal cystoid spaces in acute Vogt-Koyanagi-Harada syndrome. Am J Ophthalmol 139:670–677

Vasconcelos-Santos DV, Rao PK, Davies JB et al (2010) Clinical features of tuberculous serpiginouslike choroiditis in contrast to classic serpiginous choroiditis. Arch Ophthalmol 128:853–8

van Velthoven MEJ, Onkosuwito JV, Verbraak FD et al (2006) Combined En-Face optical coherence tomography and confocal ophthalmoscopy findings in active multifocal and serpiginous chorioretinitis. Am J Ophthalmol 141:972–975

Vance SK, Khan S, Klancnik JM et al (2011a) Characteristic spectral-domain optical coherence tomography findings of multifocal choroiditis. Retina 31:717–723

Vance SK, Spaide RF, Freund KB (2011b) Outer retinal abnormalities in acute macular neuroretinopathy. Retina 31:441–445

Verallo O, Fragiotta S, Verboschi F et al (2012) Diagnostic aspects and retinal imaging in ocular toxocariasis: a case report from Italy. Case Rep Med 2012:984512, doi.org/10.1155/2012/984512

Wickremasignhe S, Lim L (2010) Serous retinal detachment as a complication of acute posterior multifocal placoid pigment epitheliopathy. Retin Cases Brief Rep 4:129–131

Witkin AJ, Shah AR, Engstrom RE, Kron-Gray MM, Baumal CR, Johnson MW, Witkin DI, Leung J, Albini TA, Moshfeghi AA, Batlle IR, Sobrin L, Eliott D (2015) Postoperative hemorrhagic occlusive retinal vasculitis: expanding the clinical spectrum and possible association with vancomycin. Ophthalmology 122:1438–1451. doi:10.1016/j.ophtha.2015.03.016

Yamaguchi Y, Otani T, Kishi S (2007) Tomographic features of serous retinal detachment with multilobular dye pooling in acute Vogt-Koyanagi-Harada disease. Am J Ophthalmol 144:260–265

Yeh S, Wong WT, Weichel ED et al (2010) Fundus autofluorescence and OCT in the management of progressive outer retinal necrosis. Ophthalmic Surg Lasers Imaging 9:1–4

Yu S, Wang F, Pang CE et al (2014) Multimodal imaging findings in retinal deep capillary ischemia. Retina 4:636–646

Yu S, Pang CE, Gong Y et al (2015) The spectrum of superficial and deep capillary ischemia in retinal artery occlusion. Am J Ophthalmol 159:53–63